Strain partitioning on major fault zones in the northwestern Tauern Window – insights from the investigations to the Brenner Base Tunnel

Andreas TÖCHTERLE*), Rainer BRANDNER & Franz REITER

KEYWORDS

Brenner normal fault
Brenner Base Tunnel
Ahorn shear zone
Strain partitioning
Tauern Window
SEMP

Institute of Geology and Paleontology, University of Innsbruck, Innrain 52, 6020 Innsbruck, Austria;

*) Corresponding author, andreas.toechterle@uibk.ac.at

Abstract

In the northwestern Tauern Window two shear zones, which were involved in the Oligocene-Miocene exhumation of the Tauern Window, have been investigated in detail: the western termination of the Ahorn shear zone and the Tauern Northern Boundary Fault. The Ahorn shear zone is a steeply dipping, ENE-WSW striking, ductile shear zone with a sinistral shear sense. The sinistral displacement along the fault is accommodated in the west by a slightly westward plunging detachment fold – namely the Schöberspitzen antiform. The retrodeformation of this fold structure yields an accommodated offset on the Ahorn shear zone of approximately 7-12 km. Contemporaneously to the activity of the sinistral transpressive Ahorn shear zone and to the accommodating folding, normal faults were active in upper levels of the Alpine nappe stack. The Tauern Northern Boundary Fault represents one of these faults in the western Tauern Window. Today it looks like a moderately N-dipping, apparent sinistral strike-slip fault. A model is proposed whereby the Tauern Northern Boundary Fault is a rotated, initially shallow WSW-dipping normal fault. The ductile Tauern Northern Boundary Fault is therefore interpreted as an old part of the normal faulting system at the western margin of the Tauern Window, which was presumably active during an early stage of exhumation of the Tauern Window.

Im nordwestlichen Tauernfenster wurden zwei Scherzonen, die maßgeblich an der oligozänen bis miozänen Exhumation des Tauernfensters beteiligt waren, genauer untersucht: die Ahorn Scherzone, bzw. deren westliches Ende, und die Tauernnordrand-Störung. Bei der Ahorn Scherzone handelt es sich um eine steilstehende, ENE-WSW-streichende, duktile Scherzone mit sinistralem Schersinn. Der sinistrale Versatz an der Störung wird im Westen an einer flach nach W abtauchenden Detachment Falte – der sogenannten Schöberspitzen Antiform – kompensiert. Über eine Rückabwicklung dieser Faltenstruktur kann der kompensierte Versatz an der Ahorn Scherzone auf ca. 7-12 km abgeschätzt werden. Gleichzeitig mit der Aktivität an der sinistral transpressiven Ahorn Scherzone und der damit verbundenen Faltung sind in den überlagernden Einheiten des alpinen Deckenstapels Abschiebungen aktiv. Dazu gehört im westlichen Tauernfenster auch die Tauernnordrand-Störung. Heute stellt sich diese als eine mittelsteil nach Norden einfallende, scheinbar sinistrale Seitenverschiebung dar. Es wird ein Modell vorgeschlagen, wonach es sich dabei um eine rotierte, ursprünglich flach in westlicher Richtung einfallende Abschiebung handelt. Die duktile Tauernnordrand-Störung wird damit als ein alter Teil des Abschiebungssystems am Westrand des Tauernfensters interpretiert, der vermutlich während einer frühen Phase der Exhumation des Tauernfensters aktiv war.

1. Introduction

The Tauern Window (TW) is a tectonic window in the Eastern Alps, where Penninic and Subpenninic units are exposed beneath Austroalpine nappes (Fig. 1). The overall architecture can be described as an antiformal updomed nappe stack. The lowermost nappes in the core of the structure consist of detached European Basement and its Permo-Mesozoic sedimentary cover – the Lower “Schieferhülle” (LSH). The basement consists of post-Variscan granitic plutons – called “Zentralgneis” – and their host rocks. It is arranged in several antiformal domes, separated by the enveloping LSH. In the western TW there are three elongate dome-structures with ENE-WSW to NE-SW trending longitudinal axes (Fig. 1).

The LSH is represented by a nappe stack of metamorphosed and strongly folded sedimentary successions consisting of meta-conglomerates, schists, quartzites, chlorite phyllites, marbles, dolomites, and rauhwackes (weathered anhydrite- and/or gypsum bearing rocks - evaporites). The LSH can be divided into several formations. Two of them should be mentioned at this point because they represent important lithostratigraphic marker horizons. Firstly, the miscellaneous evaporitic-carbonatic-siliciclastic Aigerbach Fm., which is presumably Upper Triassic in age as indicated by the sulphur isotopes ($\delta^{34}S$) of the evaporites (Brandner et al., 2008). Secondly, the Hochstegen Fm. – calcareous and partly dolomitic marbles, which are Upper Jurassic in age (Klebelsberg, 1940; Kießling and Zeiss, 1992). The LSH represents a post-Variscan (Permian) to at least Upper Jurassic – possibly Cretaceous – transgressive to open marine succession on a subsiding continental basement. Basement rocks and LSH exhibit Oligocene amphibolite facies metamorphism (Frey et al., 1999). The units were part of the European margin during the opening of the Penninic Ocean in Jurassic time, and were later part of the lower plate during subduction of the Penninic Ocean. Presently they are in a tectonic position beneath the Penninic nappes and are therefore called Subpenninic nappes (Schmid et al., 2004).

The Penninic units or Upper "Schieferhülle" (USH) consist of detached rocks from the interior of the Penninic Ocean and its northern continental margin. The Bündnerschiefer are the main-unit of the Penninic zone in the investigation area, they represent the sedimentary and partly volcanic filling of the Penninic Ocean and consist in large part of a succession of carbonatic-siliciclastic metaarenites and metapelites. Mainly in the upper part of the Bündnerschiefer, sedimentary structures from turbiditic deposition and olistolithes of different sizes are often preserved. In the lower part of the Bündnerschiefer, small lenses of metamorphosed mafic rocks are intercalated but no remnants of an oceanic crust could be found in the northwestern TW. Here the substratum of the Bündnerschiefer consists of a succession of metamorphosed terrestrial to shallow-marine deposits, comparable with the stratigraphically lower units of the LSH. One biostratigraphically constrained date is given by crinoid stem fragments in dolomitic marbles within this succession, which are Middle Triassic in age (Frisch, 1975; Brandner et al., 2008). The presumably Upper Triassic Aigerbach Fm. (see above) is also part of this succession. Hence, in the northwestern TW the "oceanic" Bündnerschiefer have a substratum of subsided sediments on a continental margin. The detachment of the USH during Alpine nappe stacking is located within these sediments – mainly within evaporites.

The Tarntal Nappe Complex (TNC) is situated in the boundary area between the Penninic Bündnerschiefer and the superimposed Austroalpine Innsbruck Quartzphyllite Nappe Complex (IQP). The HP-metamorphic TNC consists mainly of three nappes. One of them is the ophiolitic Reckner Complex (RC) consisting of mantle rocks exhumed in Jurassic time and pelagic sediments (Meisel et al., 1997; Ratschbacher et al., 2004). Typical rocks are tectono-sedimentary ophicalcite-breccias. The other nappes of TNC are composed of Permotriassic-Jurassic shelf sediments comparable with Lower Austroalpine successions in the northeastern TW (Heidorn et al., 2003a and references therein), and breccias or megabreccias where these shelf-sediments are reworked. Austroalpine units within the TNC are interpreted by Heidorn et al. (2003a) as extensional allochthons, which were detached and partly disintegrated to breccias during Penninic rifting before coming into contact with the exhumed mantle. Due to its particular tectonic evolution, the TNC is denoted as Ultrapenninic unit – analogous to the classification of comparable units in the Central Alps by Trümpy (1992).

The Penninic nappes are overlain by the Austroalpine nappe stack, which represents detached and stacked parts of the Adriatic plate – a continental realm south-east of the Penninic Ocean (Pfiffner, 2009). In the investigation area the Innsbruck Quartzphyllite Nappe Complex (IQP) is located to the north of the TW. To the west, the Ötztal-Stubai basement complex with its Permo-Mesozoic cover and klippen of structurally higher Austroalpine nappes overlie the Penninic units separated by the W-dipping Brenner Normal Fault (BNF) (Behrmann, 1988; Selverstone, 1988).

The onset of Penninic subduction is not well constrained but it was presumably in the Cretaceous when Austroalpine units started to thrust over Penninic units, lasting until the Eocene when the Penninic Ocean was finally closed by continent-continent collision of the Adriatic plate and Europe (Wagreich, 1995 and references therein). Nappe stacking of the Penninic nappes presumably also started in the Cretaceous and took place mainly during the Palaeogene; this is indicated by some Palaeocene to Early Eocene ages which are related directly to high pressure metamorphism (Dingeldey et al., 1997; Ratschbacher et al., 2004), and Middle to Late Eocene ages which are related to the burial-exhumation switch postdating

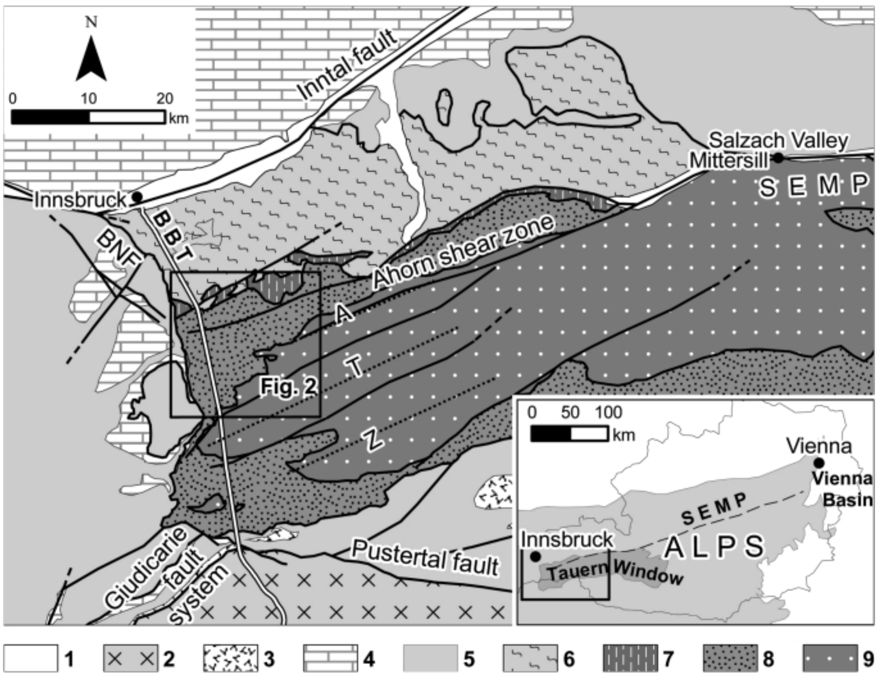

Figure 1: Tectonic sketch of the western Tauern Window (modified after Brandner 1980, Mancktelow et al. 2001, Linzer et al., 2002; Rosenberg and Schneider, 2008): 1: Quaternary cover; 2: Southalpine units; 3: Periadriatic intrusions; 4: Austroalpine Permo-Mesozoic cover units; 5: Austroalpine Paleozoic units and Austroalpine polymetamorphic basement (without IQP); 6: Austroalpine Innsbruck Quartzphyllite Nappe Complex (IQP); 7: Ultrapenninic units (including the Tarntal Nappe Complex); 8: Penninic units; 9: Subpenninic units; A: Ahorn Zentralgneis dome; T: Tux Zentralgneis dome; Z: Zillertal Zentralgneis dome; BNF: Brenner Normal Fault, SEMP: Salzach-Enns-Mariazell-Puchberg Fault, BBT: Brenner Base Tunnel.

the peak pressure conditions (Ratschbacher et al., 2004). Since the Oligocene, the Penninic-Austroalpine nappe stack has been updomed antiformally due to further contraction and the TW started to exhume (Ratschbacher et al., 1991). Ratschbacher et al. (1991) provided a model where the central units of the Eastern Alps – in particular the units of the TW – ascended and escaped to the east along major faults. In the western TW and its frame, those major faults are the W-dipping BNF and various major strike-slip faults, from N to S: the Inntal fault, the faults representing the western continuation of the Salzach-Enns-Mariazell-Puchberg fault (SEMP) (see also: Linzer et al., 2002; Rosenberg and Schneider, 2008), and the dextral Pustertal fault. A further prominent fault related to the exhumation of the western Tauern Window is suggested at its northern margin by Fügenschuh et al. (1997) and by Lammerer et al. (2008) assuming, however, differing kinematics of this fault. The denotation of the fault – Tauern Northern Boundary Fault (TNBF) – is adopted from Lammerer et al. (2008). The TNBF and the Ahorn shear zone – which is described by Rosenberg and Schneider (2008) as the western termination of the SEMP – are discussed in detail in this paper.

2. Database and methods

The geological investigations for the planned Brenner Base Tunnel are based on detailed geological mapping at 1:10 000 and 1:5 000 scales and an intensive drilling program. The drill cores are not orientated which represents a difficulty for structural interpretations. In some cases, however, the reorientation of the drill core was possible by comparing it with the sonic log (= acoustic borehole televiewer log) and the unambiguous determination of planar and linear fabrics was enabled (Decker and Reiter, 2006).

3. Deformation phases and structural features within the western Tauern Window

For a comprehensive description, the denotation and numbering of structural features should be discussed in advance. Depending on its origin, each tectonic unit was affected by multiple deformation phases resulting in superimposed structures. The following discussion covers only the post-Variscan history of several units.

3.1 Previous studies

In the following we summarize the comprehensive compilation of previous studies from Rosenberg and Schneider (2008): In all previous studies nappe-stacking and recumbent isoclinal folding occur first, whilst different authors distinguish between one (Miller et al., 1984; Selverstone, 1985; Lammerer and Weger, 1998; Rosenberg and Schneider, 2008), two (Lammerer, 1988; Kurz et al., 2001), or three deformation phases (De Vecchi and Baggio, 1982). During these phases a penetrative foliation or two consecutive penetrative foliations were developed. Afterwards during exhumation, thrusts and recumbent isoclinal folds are folded upright, connected with E-W-extension. This stage is described as one phase by De Vecchi and Baggio (1982), Kurz et al. (2001), Steffen and Selverstone (2006) and Rosenberg and Schneider (2008). Several authors differentiate between two phases during exhumation of the TW: They describe a phase of prominent upright folding followed either by “minor backthrusting” (Miller et al., 1984), by “differential uplift of TW along the Salzach fault” (Lammerer, 1988), by “extension of the western Tauern dome” (Behrmann, 1990), or by disrupting of the folded structure by strike-slip faults (Lammerer and Weger, 1998). In several studies (Selverstone, 1985; Behrmann, 1990; Kurz et al., 2001; Rosenberg and Schneider, 2008) formation of a localised foliation is described.

3.2 This study

In the LSH, as well as in the USH, there are meta-arenites and meta-conglomerates exhibiting graded bedding, and for this reason unambiguously a sedimentary fabric (S_0). Rhythmic stratification of fine-grained and medium- to coarse-grained meta-sediments in some units of the LSH, and above all in the higher parts of the Bündnerschiefer, is also considered as a primary sedimentary layering (S_0). Graded bedding and lithological stratification are nearly always parallel to the penetrative foliation (S_x) mentioned below. For the following description and discussion of the deformational features, initially a denotation by variables (x) is used which is then replaced by an absolute numbering scheme (Table 1). The numbering is related to the relative chronology of clearly identified structural features within the northwestern TW, whilst conclusions about the number of deformation phases are not drawn:

A penetrative foliation (S_x) can be seen in nearly all rocks. S_x is parallel to the axial planes of large recumbent isoclinal folds (F_x).

In the lower part of the drilling Va-B-03/04s (Fig. 2), layers with typical rocks of the LSH (non-calcareous meta-arkoses and metamorphic quartz conglomerates) are intercalated within a succession of Bündnerschiefer of the USH (calcareous phyllites, calcareous quartz phyllites, graphite phyllites). This situation is interpreted as a recumbent folding of the thrust plane between LSH and USH. The lens of LSH (“L” in Fig. 2) within the USH 2 km to the south of the drilling Va-B-03/04s can be interpreted in the same way as a recumbent isoclinal fold; the outer boundary of this lens is parallel to the metamorphic layering and the penetrative foliation Sx within the

Structures	Shearing along brittle or ductile faults	Folding	Foliation
Graded bedding, rhythmic stratification of fine-grained and medium- to coarse-grained meta-sediments			S_0
Thrust plane between LSH and USH	Sh_1		
Recumbent isoclinal folds, regionally developed penetrative foliation		F_2	S_2
Upright folds, localised foliation	Sh_3	F_3	S_3

Table 1: Relative chronology of clearly identified structural features within the northwestern TW.

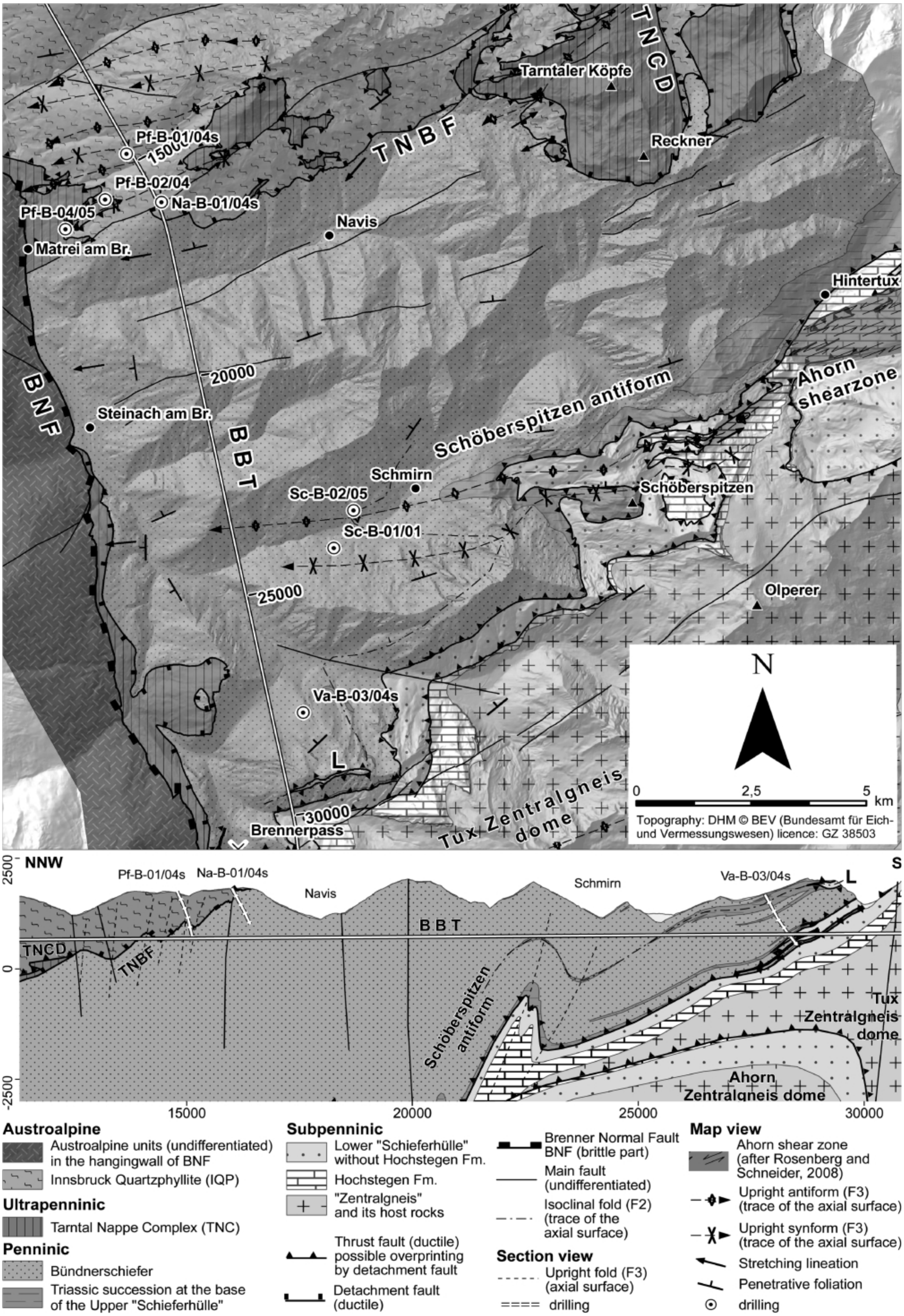
TNCD
Tarntaler Köpfe
Reckner
TNBF
Pf-B-01/04s
Pf-B-02/04
Na-B-01/04s
Pf-B-04/05
Matrei am Br.
Navis
Hintertux
20000
BNF
Steinach am Br.
Schöberspitzen antiform
Ahorn shearzone
BBT
Schmirn
Schöberspitzen
Sc-B-02/05
Sc-B-01/01
25000
Olperer
N
Va-B-03/04s
L
0
2,5
5
km
Topography: DHM © BEV (Bundesamt für Eich- und Vermessungswesen) licence: GZ 38503
30000
Brennerpass
Tux Zentralgneis dome
NNW
S
2500
0
-2500
Pf-B-01/04s
Na-B-01/04s
Navis
Schmirn
Va-B-03/04s
BBT
TNCD
TNBF
Schöberspitzen antiform
Tux Zentralgneis dome
Ahorn Zentralgneis dome
15000
20000
25000
30000
Austroalpine
Austroalpine units (undifferentiated) in the hangingwall of BNF
Innsbruck Quartzphyllite (IQP)
Ultrapenninic
Tarntal Nappe Complex (TNC)
Penninic
Bündnerschiefer
Triassic succession at the base of the Upper "Schieferhülle"
Subpenninic
Lower "Schieferhülle" without Hochstegen Fm.
Hochstegen Fm.
"Zentralgneis" and its host rocks
Thrust fault (ductile) possible overprinting by detachment fault
Detachment fault (ductile)
Brenner Normal Fault BNF (brittle part)
Main fault (undifferentiated)
Isoclinal fold (F2) (trace of the axial surface)
Section view
Upright fold (F3) (axial surface)
drilling
Map view
Ahorn shear zone (after Rosenberg and Schneider, 2008)
Upright antiform (F3) (trace of the axial surface)
Upright synform (F3) (trace of the axial surface)
Stretching lineation
Penetrative foliation
drilling

Figure 2: Tectonic map of the northwestern Tauern Window and cross section along the BBT. TNBF: Tauern Northern Boundary Fault, TNCD: Tarntal Nappe Complex Decollement, BNF: Brenner Normal Fault, L: Occurrences Lower Schieferhülle rocks within the Bündnerschiefer resulting from recumbent isoclinal folding of the nappe contact – for explanation see text.

Bündnerschiefer (see also Fig. 2). Hence there is a clear chronology of thrusting (Sh_{x-1}; "Sh" for shearing along faults) from USH onto LSH and subsequently isoclinal folding (F_x) of this thrust plane.

Metamorphic layering, recumbent isoclinal folds, and penetrative foliation S_x are arched around the Zentralgneis antiforms (F_{x+1}) and are also partly involved in subordinate upright folding. Rarely an axial surface foliation is developed (S_{x+1}). A foliation (S_{x+1}) which clearly postdates S_x can also be found within shear zones discussed below.

4. Tauern Northern Boundary Fault System

4.1 P-T-t Data

In the northwestern corner of the Tauern Window, there are four main tectonic units of the Eastern Alps adjacent to each other; these are the Penninic Bündnerschiefer, the Ultrapenninic TNC, the Austroalpine IQP and the Austroalpine Ötztal-Stubai basement complex in the hangingwall of the BNF. They all differ in their Alpine metamorphic history. The thermal peak of Alpine metamorphism and the onset of cooling of the Austroalpine units were during Late Cretaceous times (Frank et al., 1987; Fügenschuh et al., 1997; Fügenschuh et al., 2000; Heidorn et al., 2003b). Since Paleogene times, temperatures in the recently exposed parts of the Ötztal-Stubai basement complex have not exceeded 200° C (Fügenschuh et al., 2000).

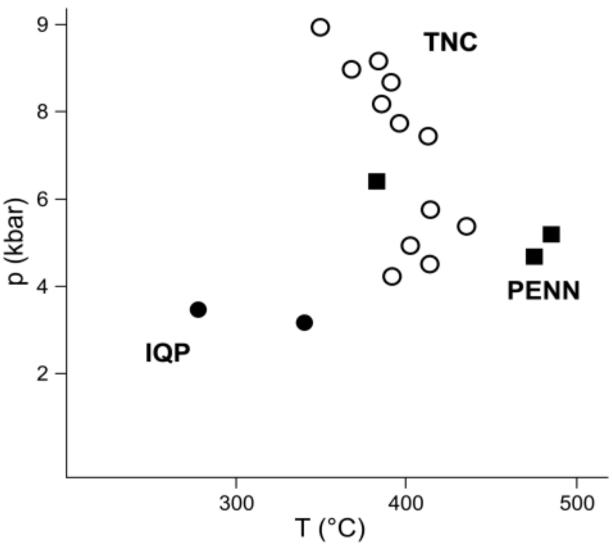

Figure 3: P-T-conditions of the units in the northwestern corner of the Tauern Window during alpine metamorphism presented by Dingeldey et al. (1997). IQP: Innsbruck Quartzphyllite Nappe Complex; TNC: Tarntal Nappe Complex; PENN: Penninic Bündnerschiefer.

The maximum Alpine metamorphic conditions of the IQP were achieved during Late Cretaceous between 83 and 77 Ma (Heidorn et al., 2003b). These reached about 4 kbar and 370° C, and until Paleogene times the temperatures have dropped below 300° C (Dingeldey et al., 1997; Fügenschuh et al., 1997). The Ultrapenninic TNC shows a HP-event with maximum pressures about 8-10.5 kbar followed by a temperature increase to 450° C (Dingeldey et al., 1997). Most ages indicate an Eocene Alpine metamorphism for the TNC (Dingeldey et al., 1997; Heidorn et al., 2003b), but also older ages around 80 Ma are suggested by some studies (Heidorn et al., 2003b; Klier, 2005). The Penninic Bündnerschiefer in the northwestern Tauern Window show maximum metamorphic conditions around 6-7 kbar followed by 500° C during Eocene times around 40 Ma (Dingeldey et al., 1997; Hoinkes et al., 1999; Heidorn et al., 2003b) (Fig. 3).

4.2 Field data

The rocks at the contact between IQP and TNC consist of rauhwackes and/or quartzites. Rauhwackes are residual rocks with a cellular texture consisting of a rust-coloured framework of calcite crystals. Breccia-type rauhwackes containing clasts and chips from the surrounding rocks are common. Quartzites are often found between rauhwackes and the IQP. Besides varying amounts of mica they also contain porphyroclasts of altered feldspar. At the contact to the IQP the quartzites show mostly a mylonitic fabric (Klier, 2005). Quartz microstructures exhibit bulging recrystallisation as well as subgrain rotation recrystallisation (Fig. 7a - c). The average particle size of the recrystallised grains is widespread, in areas with dominating subgrain rotation recrystallisation the subgrains are about 20-40 µm in size. The stretching lineation trends WSW-ENE to WNW-ESE. Although the nature of the contact between IQP and TNC is not completely clear, it is interpreted as a decollement horizon called Tarntal Nappe Complex Decollement (TNCD) (see discussion section 6.1.). The IQP is situated both below and above the TNC, as the contact consists of the same rocks in both cases, therefore it can be presumed, that the TNCD is isoclinally folded.

A further prominent fault is the Tauern Northern Boundary Fault (TNBF), which separates the Austroalpine IQP in the hangingwall from the Penninic Bündnerschiefer in the footwall. Although the TNBF is poorly exposed, the map scale trace of the fault can be determined by mapping of the adjacent tectonic units. In the area of the Reckner summit (Fig. 2), the IQP pinches out between the superimposing TNC and the underlying Bündnerschiefer so that these latter units came into contact. At this contact, none of the characteristic rocks of the TNCD (= rauhwackes or quartzites) can be observed, therefore we assume that the TNCD is truncated by the TNBF and that the TNC is also in the hangingwall of the TNBF. The Penninic Bündnerschiefer in the footwall of the TNBF contain a high amount of phyllosilicates and graphite. Typical features are a very tight foliation, an ENE-WSW striking crenulation, and ductile to semiductile shear bands. Stretching lineations at the TNBF range from E-W to ENE-WSW direction. The dataset of the BBT-investigations does not provide sufficient data to unambiguously determine the shear sense along the TNBF. However, at two outcrops a top-to-the-west movement can be determined [K631 (database entry by Decker, K.): stretching lineation: 239/15, shear sense indicator: sigma clasts; F0985:

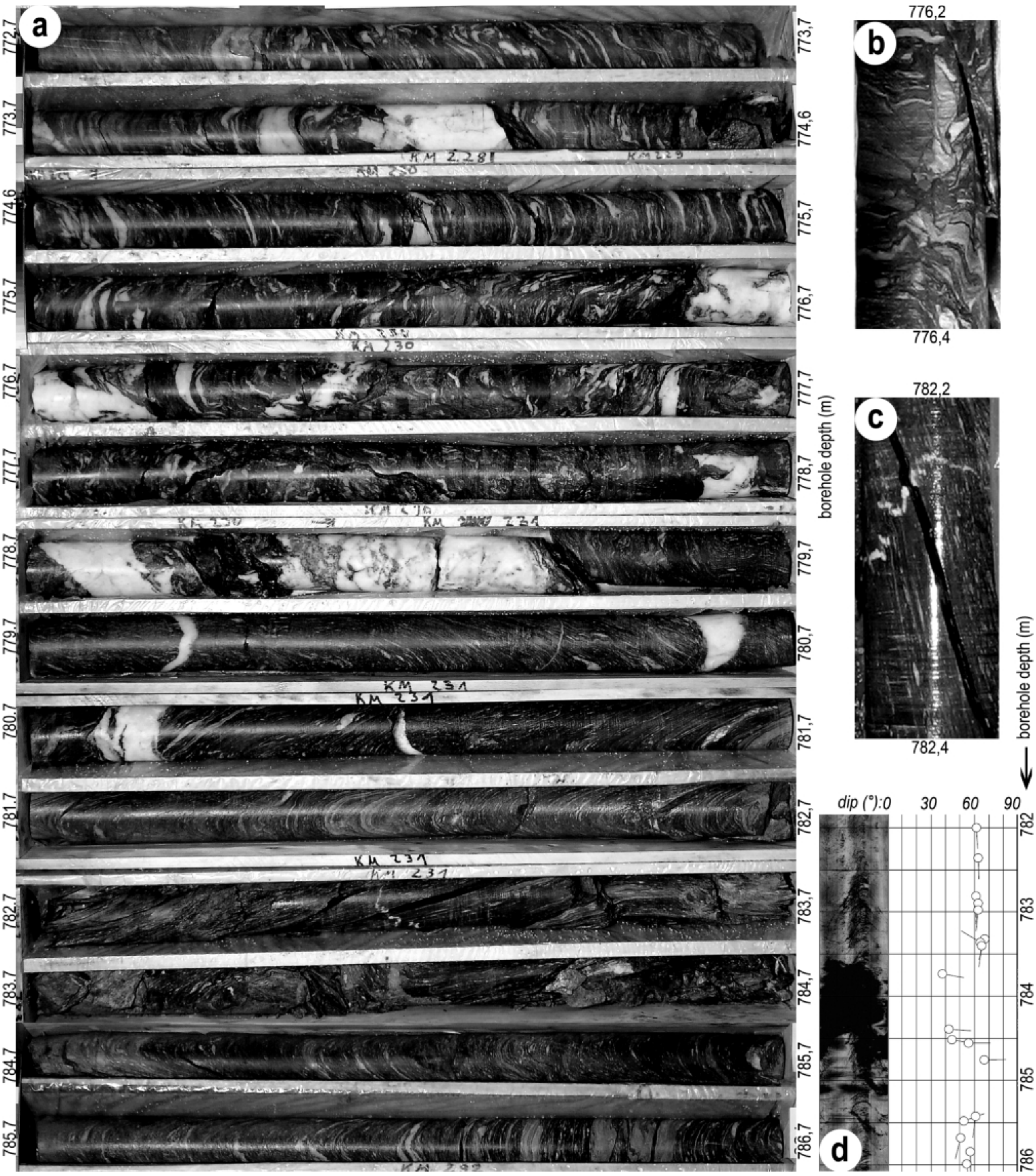

Figure 4: Drill core sections (a-c) and corresponding sonic log (d; modified after Rübel, 2006b) of Pf-B-01/04s (Photo a: Grubinger, H.): (a): The core zone of the TNBF and the IQP directly above – the IQP in the upper part of the drill core exhibits an undulating foliation (detailed view: b) whereas the rock from about 779 metres downwards is characterised by a strongly developed and regular (mylonitic) foliation (detailed view: c). There are numerous steeply S-dipping joints parallel to the mylonitic foliation, which can be identified in the drill core sample as well as in the sonic log (782.0-783.5). The orientation of the planes determined in the sonic log by Rübel (2006b) is displayed graphically in the right column of the log (d): The position of the point indicates the depth and the true dip of the plane; a position further to the right means a steeper dipping plane (from 0 to 90°). The direction of the tail indicates the direction of dip; facing upwards means a northward dip, facing to the left means an eastward dip etc. The borehole televiewer scans the borehole wall using an acoustic signal. The amplitude of the reflected signal is displayed on the uncoiled, colour-coded scan of the borehole wall. Dark colours signify low amplitudes and bright colours denote high amplitudes.

stretching lineation: 277/14, shear sense indicator: quartz fibres at a tensional stepover of C-planes]. The southern part of the IQP and the TNC in the hangingwall, the northern Bündnerschiefer, and the TNBF are additionally folded by upright

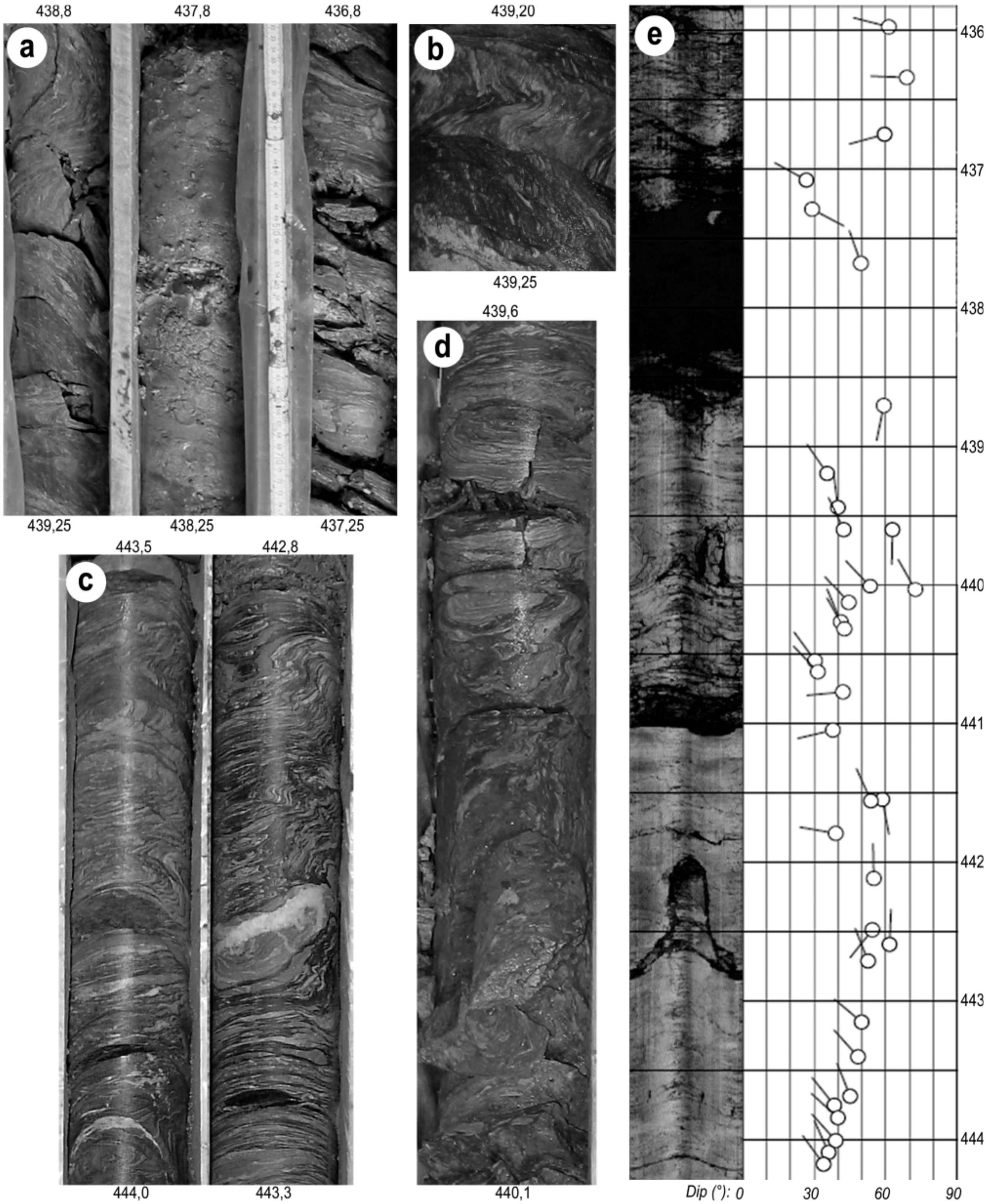

Figure 5: Drill core sections (a-d) and corresponding sonic log (e; modified after Rübel, 2006c) of Pf-B-02/04 (see Fig. 4 for a detailed explanation of the sonic log): The section is located at the TNBF. (a): Small W-dipping brittle faults above the clay gouge of the main fault give indications for the orientation of the main fault itself because they have been detected by the sonic log (e). Axial surface foliation in folded Bündnerschiefer (a-d) below the clay gouge is interpreted to be the NNW-dipping plane set in the sonic log. (b): Detailed view of section (a), pressure solution at axial surface foliation produces apparent reverse faulting offset. (c): Strong pressure solution at axial surface foliation becomes the dominant plane set and is detected by sonic log. (d) Steep dipping brittle fault allows an exact calibration of drill core samples. (Photos c & d: Grubinger, H.)

folds with E-W-trending axes, a wavelength of about 1 km, and amplitudes of 100-200 metres.

To the west – close to the BNF – the TNBF is truncated by an ENE-WSW-striking fault, which belongs presumably to a system of steep, ENE-WSW-striking sinistral brittle faults which are very common in this area (Fig. 11b).

4.3 Drillings

The four drillings described below are situated within either the Austroalpine IQP or the Ultrapenninic TNC, and they all penetrate into the underlying Penninic Bündnerschiefer.

Drilling Pf-B-01/04s: This is an inclined drilling with a drill-hole direction of 63° to SSE (150°) at the surface and 70° to ESE (119°) at the final depth of 1120 m (Rübel, 2006b). The TNBF separating IQP and Bündnerschiefer is truncated at 785 metres drilling depth, it is a ductile shear zone represented by a ca. 5 m thick mylonite with an open folded foliation and stretching lineation. A reorientation of the drill core by sonic log data (Rübel, 2006b) was possible (Fig. 4). The foliation in the long limbs of the open folds dips steeply to the S. The stretching lineation trends E-W and plunges towards WSW. The strongly foliated matrix of the mylonitic rock consists mainly of mica and graphite. Quartz-calcite-aggregates build sigmoids according to the definition of Passchier and Trouw (2005). Numerous pyrite grains provide good shear sense indicators. Fringes around pyrite grains and shear bands exhibit differing shear senses in different samples of the mylonite, indicating top-to-the-WSW movement as well as top-to-the-ENE movement (Fig. 7f, g). Dilatational cracks filled by newly crystallised calcite and/or mica are common in quartz-sigmoids (Fig. 7e). Quartz grains exhibit undulose extinction and sometimes incipient bulging recrystallisation (Fig. 7d). The average particle size of recrystallised grains is less than 10 µm.

Drilling Pf-B-02/04: The length of this drilling is 630 metres. It is a vertical drilling, but deviated slightly to ENE (70°) so that it has an inclination of 80° at the final depth (Rübel, 2006c). The drilling cuts through IQP until 438 metres drilling depth. There is a one metre thick brittle fault consisting of clay gouge, which separates the IQP from the underlying Bündnerschiefer (Fig. 5). In the drill core the fault has a dip of about 35°. The planes bordering the clay gouge are interpreted as moderately NNW-dipping at the top and moderately S-dipping at the base (Rübel, 2006c). However, there are well-defined small fault planes above and below the main fault, which dip uniformly with 40-60° toward W. Although the orientation of the brittle fault between the IQP and the Bündnerschiefer intersecting with this drilling is not completely clear, a moderate dip between 25° and 45° and a direction of dip between SSW and NNW is probable. The metamorphic layering in the topmost Bündnerschiefer is folded by recumbent – tight to isoclinals folds with a penetrative pressure solution cleavage parallel to the axial planes (i.e., an axial surface foliation). Pressure solution causes apparent offset of metamorphic layering. Apparent offset pretends downward as well as upward movement depending on the orientation of metamorphic layering in relation to the axial surface foliation (Fig. 5). The pressure solution cleavage is recorded by the sonic log. The planes dip uniformly with 30-50° towards NNW.

Drilling Pf-B-04/05: This vertical drilling has a final depth of 452 metres. It deviated slightly, so that it is inclined 8° to the east at the final depth (Rübel, 2006d). The drilling cuts across the TNC (7-249m), the IQP (249-412m), and the Bündnerschiefer (412-final depth at 452m). The TNC consists of greenschists and ophicalcite-breccias belonging to the ophiolitic Reckner Complex (7-34m), rauhwackes (34-40m), quartzites and phyllites (40-217m), and an anhydrite-succession (217-249m). Rauhwackes are comparable to those cropping out on the surface. The anhydrite-layer represents the unweathered equivalent, it consists of massive, nearly jointless anhydrite. Brittle fractures or joints at the margin of the anhydrite succession are cemented by gypsum. Dolomite clasts and chips of chloritic phyllite float within the anhydrite which represents the Tarntal Nappe Complex Decollement (TNCD). It separates the TNC from the underlying IQP. The tectonic contact between IQP and Penninic Bündnerschiefer – the TNBF – is transected at 412 metres borehole depth. No cataclastic fault rocks were observed at the contact. The dip direction of the tectonic con-

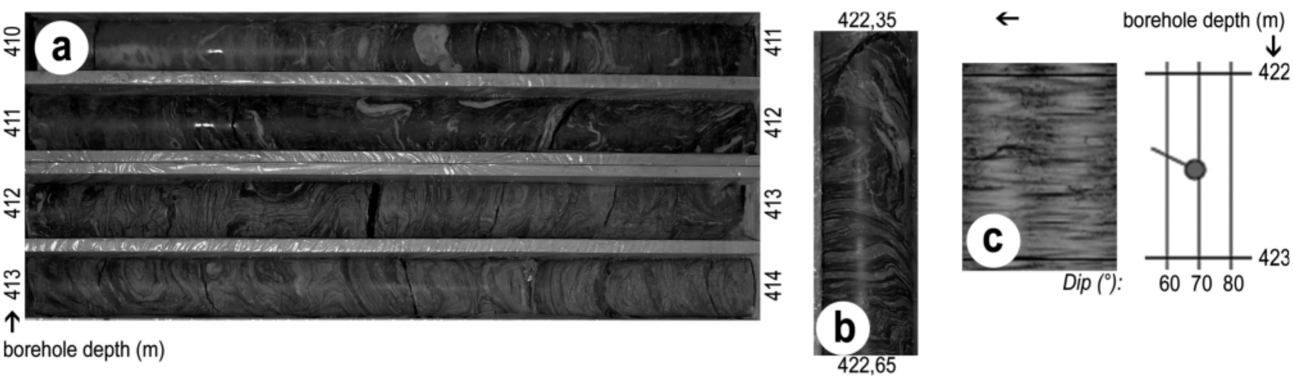

Figure 6: Drill core sections (a & b) and corresponding sonic log (c; modified after Rübel, 2006d) of Pf-B-04/05 (see Fig. 4 for a detailed explanation of the sonic log). The section is located at the TNBF: (a): Drill core section exactly at the contact of the IQP to the Bündnerschiefer exhibiting a purely ductile fault. Recumbent folding and axial surface foliation is clearly visible in Bündnerschiefer (412-414 m). (b and c): Small brittle fault enabling later reorientation and determination of axial surface foliation in drill core sample. (Photos: Grubinger, H.)

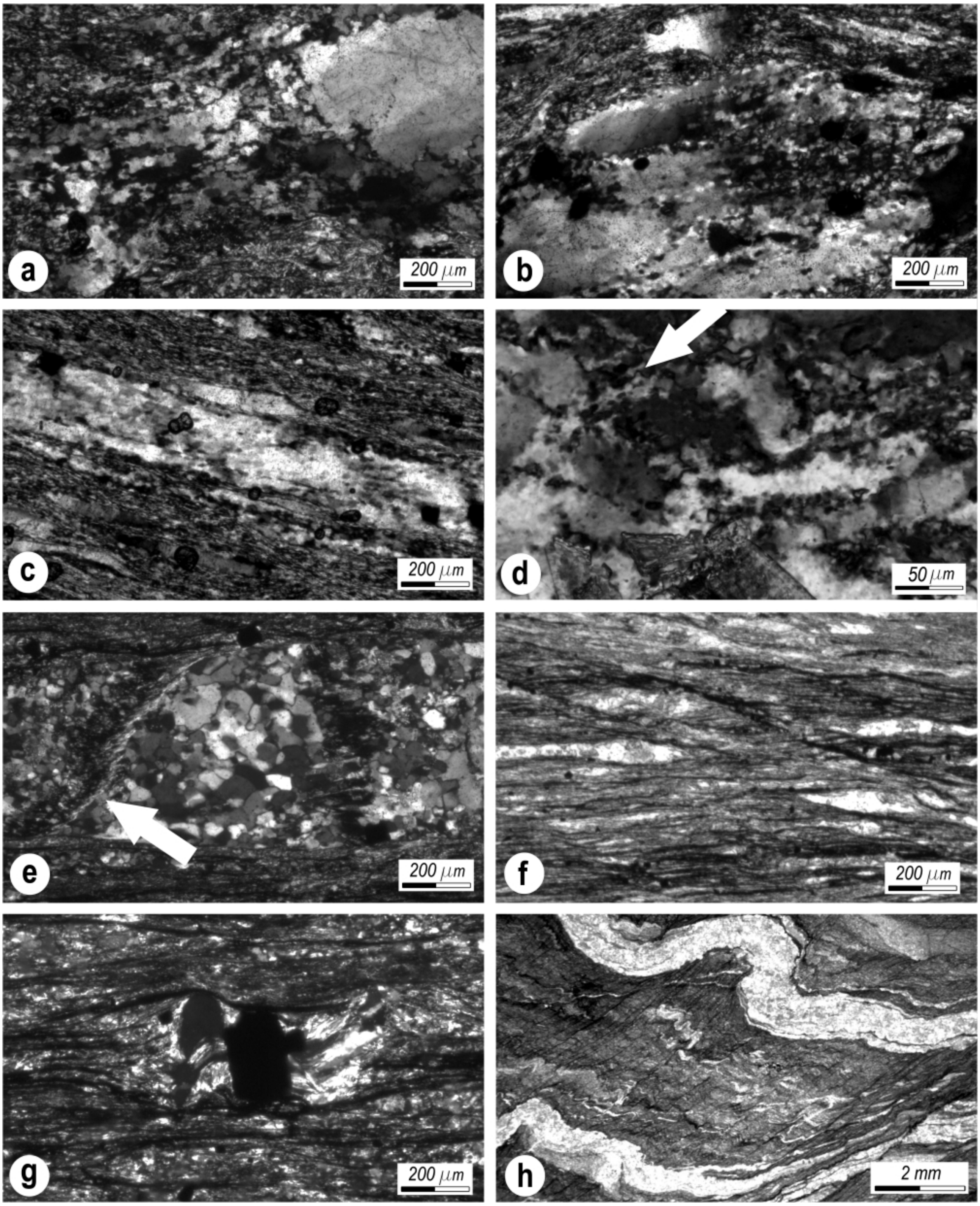

Figure 7: Thin sections from mylonitic rocks from the Tarntal Nappe Complex Decollement (TNCD) (a-c) and from the Tauern Northern Boundary Fault (TNBF) (d-h). Viewing direction is always towards north: (a): Quartzitic mylonite with dominant bulging recrystallisation (sample F0758B). (b): Quartzitic mylonite with bulging recrystallisation and incipient subgrain rotation recrystallisation; core-mantle structures are developed (sample RK310). (c): Quartzitic mylonite with dominant subgrain rotation recrystallisation within a ribbon grain; typical ribbon grains are abundant features (sample RK 310). Average particle size of recrystallised grains in quartzitic mylonites at the TNCD (a-c) is about 20-40 µm. (d): Incipient bulging recrystallisation at the TNBF; new grains are smaller than 10 µm. [The grain boundaries are cloudy because the thickness of the thin section (30 µm) is larger than the individual bulges are. A well observable bulge is marked by the arrow.] (sample SG138). (e): Tension gashes in quartz-sigmoids are cemented by calcite and mica fibres (sample SG138). (f): C´-type shear bands transecting the main foliation in mica-quartz-graphite mylonite indicate top-to-the-E shearing (sample SG138). (g): Strain fringes of quartz and mica around elongate pyrite grain indicate top-to-the-W shearing (sample SG139). (h): Axial surface foliation with a strong pressure solution in mica-quartz-calcite-graphite mylonite within the Bündnerschiefer near to the contact to IQP; lower right: axial surface foliation seems to act as C´ type shear bands (sample SG183).

tact could not be reconstructed successfully. The quartzphyllite shows nearly no evidence for intense shear deformation in contrast to the underlying Bündnerschiefer. The metamorphic layering in the topmost Bündnerschiefer is folded by recumbent folds with an intense axial surface foliation similar to that seen in drilling Pf-B-02/04. The axial surface foliation dips about 35° towards and the foliation planes seem to partly act as shear bands with top-to-the-NNE sense of shear (Fig. 7h).

Na-B-01/04s: This is an inclined drilling with drill-hole direction of 65° to S on the surface and 63° to SSE at final borehole depth (Rübel, 2006a). Several up to 10 metre thick brittle fault zones indicate a landslide in the upper 50 to 70 metres of the drilling. The tectonic contact of IQP to the Bündnerschiefer is located in the basal area of the mass movement at 66 metres drilling depth. There is a brittle fault represented by 1.5 metres of clay gouge. The sonic log suggests a steeply N-dipping fault plane, however, because of the position at the base of a mass movement it cannot be determined definitively if the brittle contact is a tectonic fault or a sliding plane of the landslide.

5. The western termination of the SEMP fault

The Salzach-Enns-Mariazell-Puchberg fault (SEMP) forms one of the most noticeable lineaments in the Eastern Alps. The entire fault zone is clearly traceable from Mittersill, in the Salzach Valley further towards the east where it extends into the Vienna Basin adjacent to the northeastern margin of the Alps (Linzer et al., 2002) (Fig.1). The activity of the fault is related to the Oligocene-Miocene lateral extrusion of the Eastern Alps, whereby mainly sinistral displacement is accommodated along the fault (Ratschbacher et al., 1991). The fault forms the northern boundary of the central part of the TW over a distance of more than 60 km along the E-W-trending Salzach valley. This part – also called Salzachtal fault – is characterised by a transition from brittle to ductile deformation mechanisms from E towards W (Wang and Neubauer, 1998). The western continuation of the Salzachtal fault is still a matter of debate. Frisch et al. (2000) and Linzer et al. (2002) assume a split into a splay of predominantly three ductile shear zones aligned along the margins of the Zentralgneis domes within the TW. Rosenberg and Schneider (2008) interpret the entire western Tauern Window as a restraining bend at the western end of the SEMP (linking their sinistral displacement to the sinistral displacement on the Giudicarie fault in the southwest of TW): The Ahorn shear zone – as a unique direct continuation of SEMP – would be part of the en-echelon arranged system of the ENE-WSW-striking sinistral fault set (Fig. 1).

The Ahorn shear zone shows a steeply dipping ENE-WSW striking mylonitic foliation (S_3 in this study; S_2 in Rosenberg and Schneider, 2008) overprinting the main foliation (S_2 in this study; S_1 in Rosenberg and Schneider, 2008). Sense of shear indicators document sinistral displacement. Besides the Ahorn Zentralgneis dome, the fault also affects the envelo-ping units of the LSH. It terminates to the west in the border area between the LSH and the USH south of Hintertux (Fig. 2) where the sinistral displacement would be compensated by upright WNW-ESE trending folds (Rosenberg and Schneider, 2008). An increase in temperature during deformation from about 300° C at the northern margin of the shear zone to about 500° C at the southern margin can be deduced from the different deformation mechanisms of quartz and feldspar, which indicate, additionally to the sinistral displacement, a vertical displacement of about 7 km across the fault (assuming a geotherm of 30° C/km) (Rosenberg and Schneider, 2008).

5.1 Field data

5.1.1 Map-scale structures

During the investigations for the Brenner Base Tunnel no fault could be identified to be considered as a western continuation of the Ahorn shear zone within the Bündnerschiefer of the USH. This means that neither a zone with a foliation S_3 overprinting the foliation S_2, nor other ductile fabrics indicating a steep dipping sinistral shear zone, nor any larger brittle faults have been identified yet in the continuation of the Ahorn shear zone. It should be noted, however, that the identification of a ductile Sh_3-shear zone within the Bündnerschiefer is difficult and an unambiguous determination of an overprinting foliation S_3 would only be possible if it differs clearly in orientation from S_2.

The following units are located at the western end of the Ahorn shear zone (Fig. 2): The Ahorn Zentralgneis dome, including the enveloping LSH, is enveloped by a lamella of the southerly adjacent, structurally higher Tux Zentralgneis dome. The Tux Zentralgneis dome also has a hull of rocks of the LSH structurally overlain by the USH. The large-scale metamorphic layering between the Zentralgneis domes and the IQP in the northwestern TW dips moderately N to NW, however metamorphic layering and foliation S_2 are folded by upright F_3-folds at different scales. One of these folds is the Schöberspitzen antiform (Fig. 2) which is a tight to isoclinal upright antiform of LSH and the overlying USH. The main structure yields a vertical height of about 1.5 km, with parasitic folds at all scales. The fold axis of the S-verging antiform dips with 15 to 20° W and the axial plane dips steeply N. The map view exhibits a detachment fold with the Hochstegen Fm. in the core of the fold. The rocks of LSH are detached from their basement which is not involved in detachment folding. In the USH the fold structure can be tracked mainly by the Aigerbach Fm. at the base and in a marker horizon within the USH. The Schöberspitzen antiform can be detected by changes in orientation of S_2 until 2 km east of the Brenner Normal Fault (BNF) (Fig. 2).

5.1.2 Structures in outcrop-scale

At the base of the Schöberspitzen detachment fold the penetrative foliation and the metamorphic layering of the LSH dips moderately towards NW (Fig. 11e). East of the Schöberspitzen antiform the stretching lineations and the fold axes of isoclinal folds plunge gently towards WSW, and gently towards

ENE in the core of the fold (Fig. 11f). The fold axes of asymmetric, non-isoclinal folds exhibit an average plunge towards WNW with a broad distribution (from N- to WSW-plunging axes); counterclockwise folds (s folds – see Fig. 8) predominate clearly (Fig. 11f). All fold axes plot along a great circle ± parallel to the orientation of the metamorphic layering of the LSH and its basement (Fig. 11e, f). These different types of folds are interpreted as the result of progressive deformation: Layer-parallel, top-to-the-WSW directed simple shear within the NW-dipping LSH produces predominantly counterclockwise F_3-folds (and subordinately clockwise folds) with NNW-plunging fold axes (Fig. 8a) which are continuously rotated into the shearing direction while the folds become tighter and finally isoclinal (Fig. 8b).

In the Hochstegen Fm. in the core of the Schöberspitzen antiform detachment folds (F_3) at different scales are very common (Fig. 9). Their amplitude increases from the core to the external parts of the fold (Fig. 9). Different hybrid types between detachment folds and fault propagation folds with semiductile to ductile ramps are also very common. Also in these cases either the amplitude increases from the core to the external parts of the fold (Fig. 8d) or the displacement increases along the ramp in the direction of transport (Fig. 9b). Another commonly observed feature is a hinge collapse which develops in the upper parts of the folds (Fig. 9c). Fig. 9d exhibits a structure where a steep ramp is developed above a hinge collapse of a small fold. Fold structures with maximum fold amplitudes from a few centimetres to about 50 metres can be

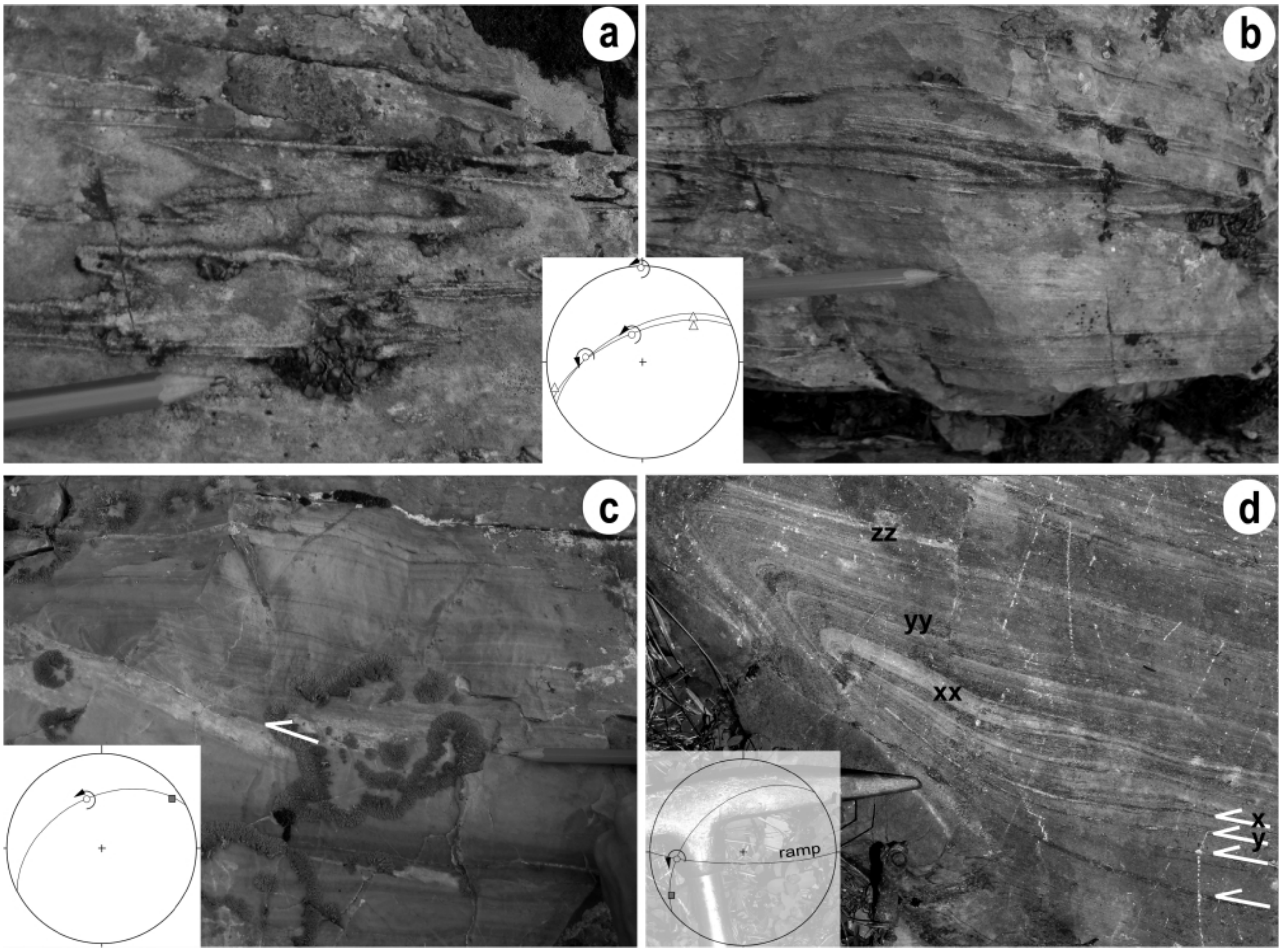

Figure 8: Different fold geometries within the NW-dipping Hochstegen Fm. in the core of the Schöberspitzen antiform (a, b, c) and slightly east of it (d). The folds in (a) and (b) are interpreted as the result of layer-parallel top-to-the-WSW directed simple shear and the structures in (c) and (d) document how layer-parallel simple shear is transferred into (initial) upright folding. The viewing direction is always towards WNW. (stereoplots: great circles: metamorphic layering and parallel penetrative foliation; circles: fold axes of vergent folds – the vergence is indicated by the rotation direction looking down the plunge of the hinge line; triangles: fold axes of very tight to isoclinal folds; full squares: stretching lineation). (a): Tight, W-verging, counterclockwise folds with N- and W-plunging fold axes. (b): Very tight to isoclinal folds with ENE-WSW-striking fold axes (see text for further explanations). (c): Tight WSW-verging fold above a ramp (white arrow) which emanates from a shear plane parallel to the metamorphic layering/penetrative foliation (along the pencil). (d): S-verging fault propagation fold with steep E-W-striking ramps emerging from the penetrative foliation which is parallel to the metamorphic layering. Four of these shear planes becoming ramps are marked by white arrows. Two of them are additionally labelled by letters (x, y) and marker horizons are labelled by double letters (xx, yy, zz). The marker horizon “xx” is folded above the shear plane “x” and the shear plane “x” ends immediately left of the fold – the marker horizon “yy” is not cut by shear plane “x”. The same applies to the marker horizon “yy”and the shear plane “y” etc. Hence, cumulative layer-parallel simple shear is accommodated by a fault propagation fold with an amplitude which increases from the core (xx) to the external part of the fold (zz). The direction of shearing along the metamorphic layering in (c) and (d) is indicated by ENE-WSW-striking stretching lineations.

observed in outcrops of the Hochstegen Fm. All these structures can be generated by accommodation of homogeneous simple shear within a metamorphic layer or a stack of layers where the amount of shortening increases upwards along the axial plane of a fold or along a ramp.

In the Schöberspitzen fold structure the structurally higher units of LSH and the lower units of USH (i.e. Aigerbach Fm.) exhibit interference patterns of F_3-folds with predominantly NW/N-plunging hinge lines and folds with predominantly E-W-striking hinge lines (Fig. 10). The stereoplot shows a broad scattering of the F_3-fold axes whereby a W-plunging maximum is clearly recognisable (Fig. 11i). In the upper and western part of Schöberspitzen antiform, similar to the main part of USH, the arrangement of F_3-fold axes yields a relatively homogeneous pattern with predominantly E-W-to ENE-WSW-striking fold axes (Fig. 11h).

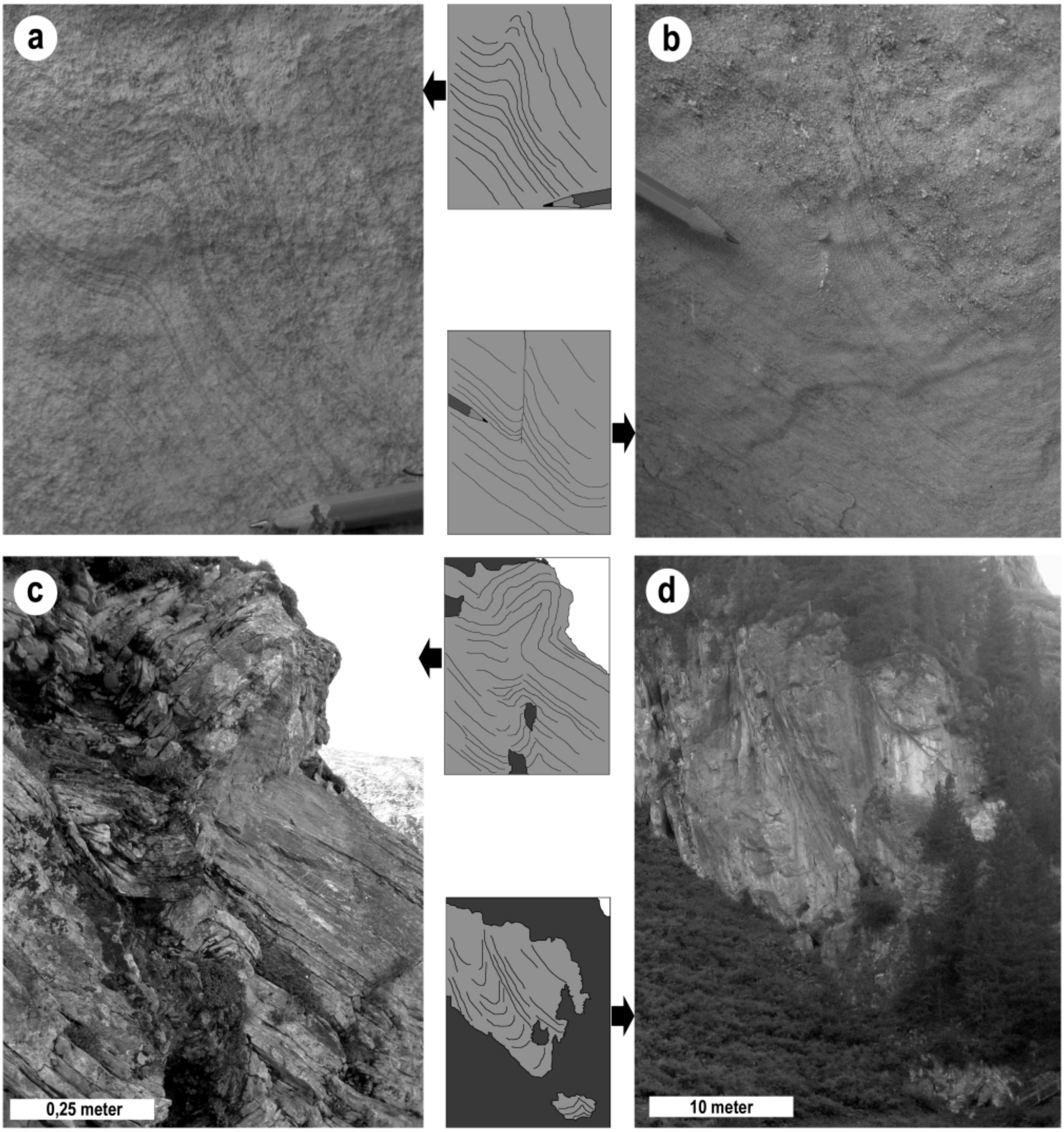

Figure 9: Structural features within the core of the Schöberspitzen antiform, viewing direction is always towards NNW. (a): Small-scale WSW-verging detachment fold resulting from homogeneous simple shear without a basal decollement. Fold amplitude grows upwards. Layer thickening in the fold hinge can be observed clearly. (b): Steep ramp (Top to WSW) resulting from homogeneous simple shear. There is no basal flat. The strain accumulated along the ramp; the displacement increases along the ramp from zero in the direction of transport. (c): Mesoscale WSW-verging detachment fold with an upwardly increasing amplitude. (d) Large scale WSW-verging detachment fold with an upwardly increasing amplitude. In the upper part a steep ramp is developed.

Figure 10: Dome-basin interference pattern of F_3-folds on the Schöberspitzen summit. The viewing direction is towards ESE (Photo: Pliessnig, H.).

6. Discussion

6.1. Tauern Northern Boundary Fault System

The quartzite at the base of the Tarntal Nappe Complex (TNC) cannot be definitively distinguished from quartzites within the TNC, which can be interpreted as part of a transgressive succession due to the occurrence of quartzitic meta-conglomerates. In the quartzites at the TNC-IQP contact a mylonitic texture is very common, thus an interpretation as a decollement horizon is possible, however, this is not confirmed. By contrast, the interpretation of the evaporite rocks occurring between the IQP and the TNC as fault rocks is unambiguous. At geologically relevant strain rates (between 10^{-14} and 10^{-10} sec^{-1}) anhydrite typically starts to flow at temperatures above 180 or 220° C, respectively (Müller and Briegel, 1978). The presence of fractured fragments from other rocks within the massive anhydrite indicates tectonic fracturing of surrounding rocks while the anhydrite was ductilely deformed. The timing of the TNCD and the relationship between the anhydrite and the quartzite mylonites is not yet clear. Quartz microstructures allow an estimation of temperature during deformation with consideration of strain rates (Stipp et al., 2002b, a). The microstructures indicate deformation in the transition zone between bulging recrystallisation and subgrain rotation recrystallisation. The strain rate is hard to evaluate, but for a relatively low average geological strain rate of 10^{-13} sec^{-1} a temperature in the range of 370° C can be deduced (for strain rates around 10^{-12} sec^{-1} temperature estimation exceeds 400° C) (Stipp et al., 2002a). Therefore the temperature during the activity of at least the quartzitic part of the TNCD was possibly just slightly lower than the maximum temperature of the TNC during Alpine metamorphism (450° C – see section 4.1.).

The TNCD is cut by the TNBF between the Penninic Bündnerschiefer and the IQP. Two BBT-drillings (Pf-B-01/04s, Pf-B-04/05) have provided a complete section across the ductile TNBF. Mylonites from the TNBF contain a high amount of mica and graphite which form the matrix and accommodate the main part of the deformation. However, the observed quartz microstructures described above indicate deformation at the frictional-viscous transition of quartz which occurs at a temperature range from 250 ± 20° C to 310 ± 30° C (Stipp et al., 2002b).

Taking into account only the metamorphic peak conditions, a drop of at least 2-3 kbar from the footwall to the hangingwall during the Alpine metamorphic history is recorded across the TNBF (Fig. 3). From this a difference in the overburden depth of about 7.5 to 11 km can be inferred assuming an average lithostatic gradient of 0.27 kbar/km. One possibility to explain this metamorphic jump is normal faulting along the TNBF. In view of the fact that the metamorphic peak conditions in the hangingwall (during Late Cretaceous times in IQP) were achieved much earlier than in the footwall (during Paleogene times in the Penninic Bündnerschiefer), and that these were even lower when the fault would have been active (see below), the actual vertical displacement could be even higher than the assumed 7.5 to 11 km. However, the present day geometry of the TNBF – a generally NNW-dipping surface which is folded by E-W-striking folds and E-W to ENE-WSW-striking stretching lineations without a significant plunge – is not that of a normal fault.

A further possibility would be an interpretation of the TNBF as oblique sinistral strike-slip fault linked to the Brenner Normal Fault as suggested by the model of Fügenschuh et al. (1997). In this model, the exhumation in the western TW can be separated into two phases: In a first phase, the Ötztal-Stubai complex and the IQP form the hangingwall and the Penninic and Subpenninic units the exhuming footwall. A roughly E-W-striking oblique sinistral shear zone linked to the W-dipping Brenner Normal Fault would be active at the northern margin of the western Tauern Window during this stage. In the second phase, the IQP belongs to the footwall as well, and no major vertical displacement at the northern margin of the western Tauern Window is expected. Even if Fügenschuh et al. (1997) do not define the oblique sinistral shear zone at the northern margin of the Tauern Window in detail, the TNBF would be a capable candidate. If the BNF and the TNBF were kinematically linked over a specific period, then during this period the absolute displacement along the specific faults should be the same at their junction. For the central part of the BNF in the area of the Brennerpass (Fig. 2), a total of 50 to 70 km absolute displacement was calculated by Fügen-

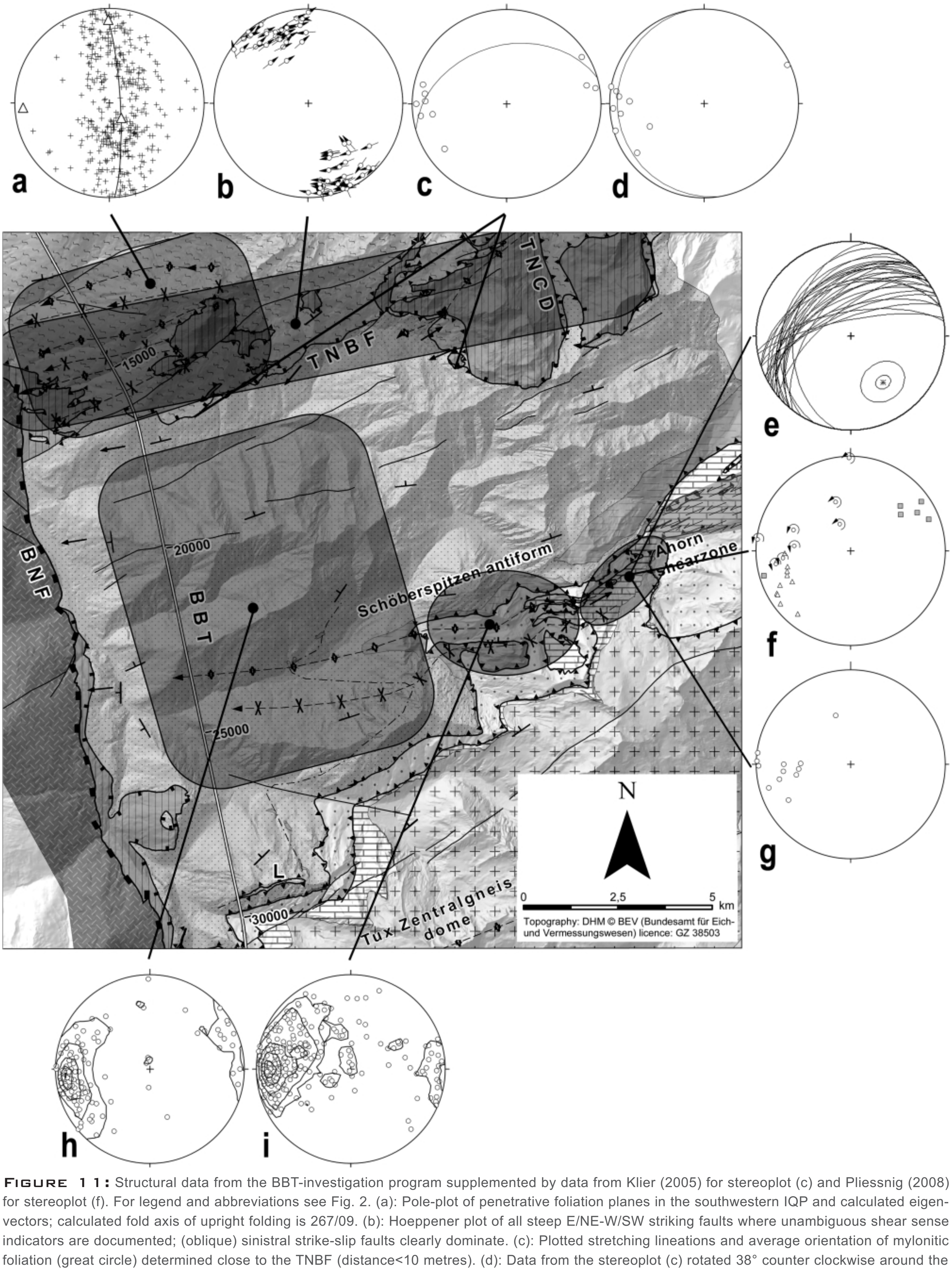

Figure 11: Structural data from the BBT-investigation program supplemented by data from Klier (2005) for stereoplot (c) and Pliessnig (2008) for stereoplot (f). For legend and abbreviations see Fig. 2. (a): Pole-plot of penetrative foliation planes in the southwestern IQP and calculated eigenvectors; calculated fold axis of upright folding is 267/09. (b): Hoeppener plot of all steep E/NE-W/SW striking faults where unambiguous shear sense indicators are documented; (oblique) sinistral strike-slip faults clearly dominate. (c): Plotted stretching lineations and average orientation of mylonitic foliation (great circle) determined close to the TNBF (distance<10 metres). (d): Data from the stereoplot (c) rotated 38° counter clockwise around the average fold axis of upright folds within IQP (267/09, see stereoplot a). (e): Mylonitic foliation at the base of the Schöberspitzen antiform (great circles) and pole of calculated mean value (= orientation of the detachment horizon: 325/50). (f): Plot of stretching lineations and fold axes of isoclinal folds within the core of the Schöberspitzen antiform (squares) and those east of it (triangles), and fold axes of vergent F_3-folds (circles) – the vergence is indicated by the rotation direction looking down the plunge of the hinge line. (g): Fold axes of detachment folds within the core of the Schöberspitzen antiform. (h): Lineation and contour plot of F_3-fold-axes within the Bündnerschiefer, data in the vicinity of nappe contacts (TNBF and BNF) are not plotted. (i): Lineation and contour plot of F_3-fold-axes within the Schöberspitzen antiform.

schuh et al. (1997). However, the offset which would have to be accommodated by the TNBF should be remarkable lower because the kinematic linkage should exist only during the first exhumation phase and because displacement decreases along the BNF from the central part of the Tauern Window towards N (and towards S) (Rosenberg and Garcia, in press). A simple geometric reconstruction yields a rough estimation for the minimum value of the rake (or pitch) of stretching lineation upon the foliation in the range of 25° (assuming a relative exhumation of 10 km, a maximum absolute offset of 50 km, and a 30° inclined TNBF striking normal to the BNF). Although the rake of stretching lineation can be altered by assuming different values for the variables, it is obvious that a significant amount should remain. In particular, a lower absolute offset would amplify the rake of the stretching lineation. In fact, the mean of the evaluated rake values of stretching lineations upon the foliations at the TNBF is at most 10° (Fig. 11c). Thus, it seems to be rather unlikely that the TNBF was an oblique sinistral strike-slip fault linked to the Brenner Normal Fault over a specific period during the exhumation of the Tauern Window.

An alternative model for the structural evolution of the TNBF is a rotation of the fault subsequent to the normal faulting activity. Large-scale northward to north-westward tilting of the Penninic units in conjunction with the superimposing Austroalpine units (and the surface in between) in the northern limb of the antiformal updomed units of the Tauern Window (Fig. 1 and Fig. 2) is described by Rosenberg and Garcia (in press). The assumption that the TNBF is tilted as a whole by upright folding subsequent to faulting is supported by the fact that the fault is folded by south-verging upright folds with wavelengths of km-scale (Fig. 2) which are potentially parasitic folds of the large-scale "Tauern Window antiform". The fold axes of these folds provide, therefore, also a possible indicator for the rotation axis of the tilted TNBF; foliations exhibit a great circle distribution indicating cylindrical folds with E-W-trending axes (Fig. 11a). Based on these assumptions the northern limb of the "Tauern Window antiform" can be backrotated in order to determine the orientation of the TNBF before upright folding. If the foliation and stretching lineation dataset from the TNBF is rotated by 38° (the average dip of foliation on the TNBF) around the average fold axis of the parasitic folds (267/09; counterclockwise rotation looking down the plunge), then a pattern of slightly WSW-dipping planes and stretching lineations (dip slip) is revealed. If the few top-to-the-W shear-sense indicators determined at the TNBF are backrotated in the same way then a top-to-the-WSW directed normal fault is indicated. From these structural considerations, it can be reasoned that the TNBF was originally probably a WSW-dipping normal fault representing an old part of the normal faulting system at the western margin of the emerging Tauern Window. In the course of amplification of the TW the TNBF was increasingly tilted and upright folded and major activity on the TNBF was terminated (Fig. 12).

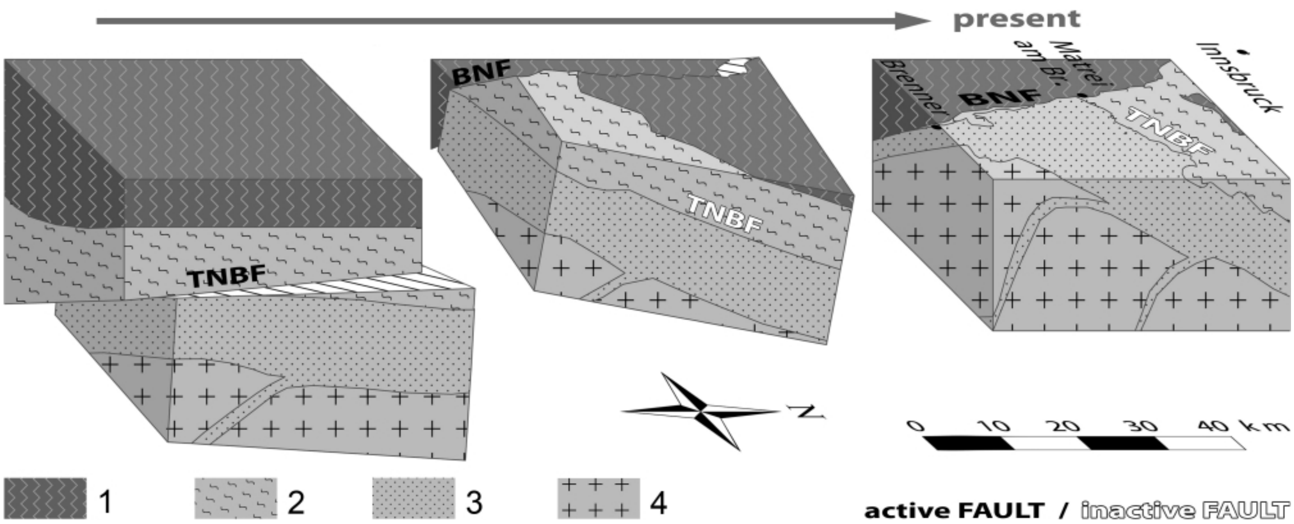

Figure 12: Schematic sketch of the tectonic evolution at the northwestern corner of the Tauern Window in respect of its exhumation. 1: Ötztal-Stubai basement complex including its Permo-Mesozoic cover and corresponding units; 2: Innsbruck Quartzphyllite Nappe Complex and Tarntal Nappe Complex; 3: Upper and Lower Schieferhülle; 4: Zentralgneis and its host rocks; TNBF: Tauern Northern Boundary Fault; BNF: Brenner Normal Fault. The TNBF is interpreted as an old rotated part of the normal faulting system at the western margin of the Tauern Window.

An absolute upper limit for the age of normal faulting activity on the TNBF is given by the thermal peak of metamorphism of the Bündnerschiefer in the footwall of the fault which occurred around 40 Ma (Dingeldey et al., 1997; Heidorn et al., 2003b). It is probable that the fault was active during an early stage of exhumation of the Tauern Window in the Late Oligocene-Early Miocene (von Blanckenburg et al., 1989: 20 Ma; Frisch et al., 2000: 23 Ma; Selverstone et al., 1995: ≤ 30 Ma). The jump in zircon fission track ages across the northern boundary of the western Tauern Window with ages between 56 and 68 Ma in the hangingwall and ages between 16 and 22 Ma in the footwall (Fügenschuh et al., 1997; Most, 2003) suggests normal faulting activity along this boundary, at least during Early Miocene times. A minimum age of activity on the TNBF is defined by the analogous ages of apatite fission tracks in the footwall and the hangingwall, however just three apatite fission track data at the western margins of the TW and IQP can be found in the literature (Grundmann and Morteani, 1985; Fügenschuh et al., 1997): Two ages in the northern area of the IQP (13 and 14.3 Ma) and one age (9 Ma) about 12 km south of the TNBF within the Bündnerschiefer. There are more data from the central and eastern part of the IQP and to the south of it, where no jump in apatite fission track ages can be recognised across the TNBF (Most, 2003); these data range from 10 to 14 Ma. It can therefore be deduced that at least from this time onwards, no major vertical displacement along the TNBF is identifiable. The IQP came into the footwall of the BNF (Fig. 1) and the IQP and Penninic Bündnerschiefer were exhumed together.

Normal faulting along the BNF continued until recent times as indicated by seismicity and GPS data (Reiter et al., 2005).

6.2 The western termination of the SEMP fault

At the western margin of the TW the Zentralgneis domes plunge to WSW beneath the BNF. The rocks of the LSH and USH envelope the ellipsoid shaped Zentralgneis domes, therefore the map view from the BNF about 30 km to the east can be treated as a stretched section view, whereby the deepest parts outcrop in the east. The Schöberspitzen antiform is located on the eastern edge of the investigation area for the BBT. In the core of the fold there are small and mesoscale structures, where homogeneous layer-parallel sinistral simple shear is accommodated by different types of upright folds (see section 5.1.2, Fig. 8c, d and Fig. 9). Because no basal decollement leading to one (or two) huge antiform(s) can be identified, it is assumed that the Schöberspitzen detachment fold is actually a bulge accommodating homogeneous layer-parallel sinistral simple shear at a large scale resulting from the total sum of the small and mesoscale structures each accommodating a portion of the shear. The sense of shear in the NNW-dipping Hochstegen Fm. is predominantly top-to-the-WSW and changes from slightly normal west of the Schöberspitzen antiform to slightly reverse in the core of the fold as indicated by stretching lineations and axes of small scale isoclinal folds (Fig. 11l). The displacement vectors of particles are therefore predominantly sub-horizontal. In the nucleus of the fold there is a bend of about 40°. East of this bend the displacement vectors of the northern block plunge slightly down towards WSW (Fig. 11f), and west of it they exhibit slight upward movement. The slightly WSW- to W-plunge of the fold axis of the main structure is primarily considered as a consequence of detaching from the moderately NNW-dipping basement. Due to the sub-horizontal displacement vectors of particles, the Schöberspitzen antiform is interpreted to be a W-verging structure rather than a S-verging one. About 1 km northeast of the core of the Schöberspitzen antiform, the western end of the Ahorn shear zone is described by Rosenberg and Schneider (2008) to be located within the Hochstegen Fm. (Fig. 2). For these reasons we postulate that the Schöberspitzen antiform accommodates the main part of sinistral simple shear of the Ahorn shear zone and represents the western termination of the SEMP. Rosenberg and Schneider (2008) propose WNW-trending upright folds west of the end of the Ahorn shear zone to accommodate sinistral shear, however, the published site locations of WNW-trending folds plot mainly in the USH whereas the end of Ahorn shear zone is located in the LSH. The shear zone would thus have to cross the LSH-USH nappe contact, but no significant folding or offset of this older fault is detectable. A large amount of shear deformation can however be accommodated in the Schöberspitzen antiform, which has its nucleus in the LSH directly in continuation of the Ahorn shear zone.

The retrodeformation of the Schöberspitzen detachment fold should deliver an assessment of the displacement along the Ahorn shear zone which is accommodated by this fold. For the retrodeformation of the Schöberspitzen detachment fold the two-dimensional method of equal-area restoration is used (Mitra and Namson, 1989). This means that the folded Hoch-

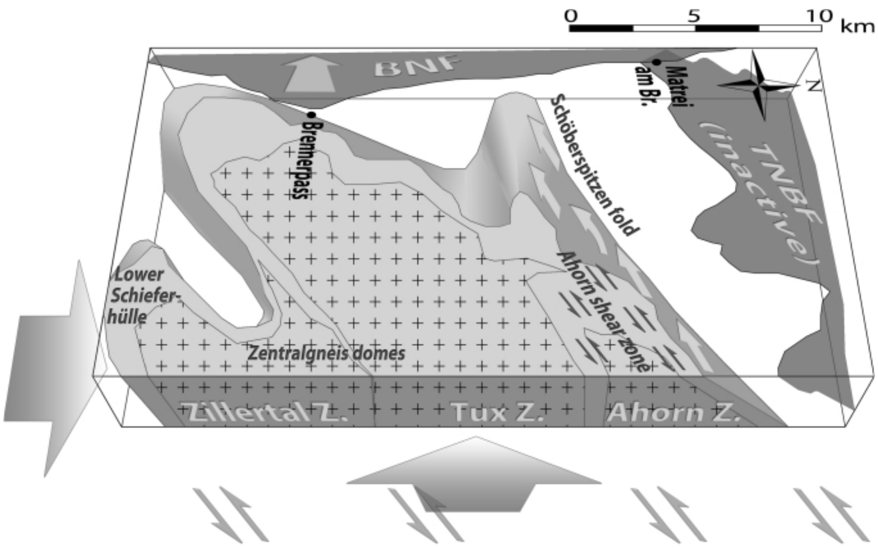

Figure 13: Schematic sketch of the kinematics during the exhumation of the western Tauern Window at a late stage. Note the linkage between the ENE-WSW-striking sinistral Ahorn shear zone running along the ENE-WSW-trending Ahorn Zentralgneis dome and the W-plunging Schöberspitzen detachment fold. Arrows on the top of the Lower Schieferhülle indicate the displacement vectors of particles within the LSH in respect to the Zentralgneis. The strike-slip symbols at the bottom of the figure symbolise that sinistral shear is not restricted to the Ahorn shear zone. BNF: Brenner Normal Fault; TNBF: Tauern Northern Boundary Fault; Z.: Zentralgneis dome.

stegen Fm. is retrodeformed to its undeformed state related to the upright folding whereby its area in the section remains constant during retrodeformation (Fig. 14d). Hence, this method presumes plane strain and constant rock volumes during folding. No features can be observed which indicate an increased pressure solution in the realm of the Schöberspitzen antiform. This would lead to a reduction in the folded rock volume and as a consequence of this to an underestimation of accommodated shear. For the retrodeformation the well-defined antiform of Hochstegen Fm. is projected along the fold axis vector (268/25) onto a plane (128/41) parallel to the average stretching lineation (060/18) and normal to the orientation of the detachment horizon (= boundary surface of Tux Zentralgneis body and metamorphic layering in the lowermost Hochstegen Fm.: 325/50) (see Fig. 11e). The projection plane should be parallel to the plane of strain (= the plane spanned by the principal strain axes X and Z) of the Schöberspitzen fold. It is not parallel to the plane of strain within the Ahorn shear zone because of the deviating shear direction, but it is still normal to the metamorphic layering. The projection (Fig. 14b) reveals that the Schöberspitzen structure consists not just of a single pair of two major tight to isoclinal folds, it is

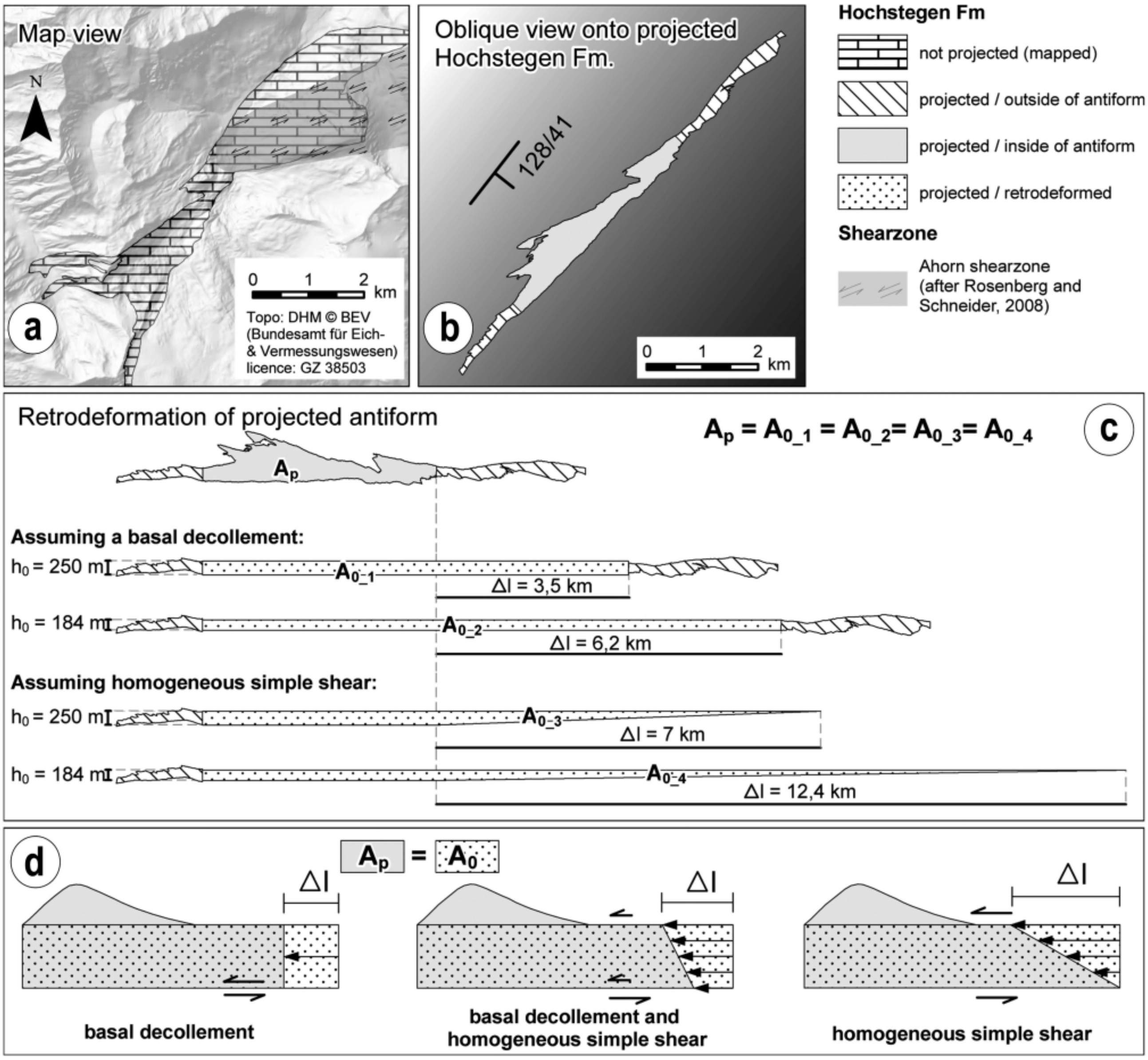

FIGURE 14: Map view shows Hochstegen Fm. in the realm of Schöberspitzen antiform at the western end of Ahorn shear zone. (b) Oblique cross section: The mapped Hochstegen Fm. is projected onto a plane (128/41) which is parallel to the average stretching lineation in the core of the fold (060/18) and normal to the orientation of the detachment horizon (= boundary surface of Tux Zentralgneis body and metamorphic layering in lowermost Hochstegen Fm.: 325/50). The viewing direction of the oblique view is normal to the projection plane; the projected Hochstegen Fm. is not contorted. (c): The different results of retrodeformation are based on various assumptions concerning the folding mechanism outlined in (d) and on differing prefolding thicknesses of the Hochstegen Fm. which represents the detachment horizon. 250 metres is based on some auxiliary sections across the Hochstegen Fm. in this area, and 188 metres is the average thickness of projected Hochstegen Fm. adjacent to the antiform. (d): Models for equal-area restoration of detachment folds differing in the percentage of homogeneous simple shear within the detachment horizon. Δl: the shortening of the uppermost layer = the accommodated displacement along the shear zone; A_0: area before the deformation; A_p: area after the deformation.

instead a broad thickening of the Hochstegen Fm. with parasitic tight to isoclinal verging folds at different scales, which is in accordance with the observations in the field as described above. Furthermore, an average thickness of the Hochstegen Fm. of about 184 m outside of the Schöberspitzen fold can be deduced from the projection. Some auxiliary cross sections indicate instead a greater average thickness of about 250 m of the Hochstegen Fm. The retrodeformation has to take into account the assumed deformation model for the detachment fold, where the strain is distributed homogeneously over the whole Hochstegen Fm. without a basal decollement. In fact, the detachment horizon is represented by the whole Hochstegen Fm. Its internal deformation has an essential influence on the results of the retrodeformation of the Schöberspitzen antiform concerning the accommodated shear which corresponds to the shortening of the uppermost layer within the Hochstegen Fm. (Δl in Fig. 14c, d). The largest value results from the model without shear along a basal decollement as supposed for the Schöberspitzen fold. With these assumptions and parameters, the retrodeformation of the Schöberspitzen antiform yields an accommodated displacement on the Ahorn shear zone of approximately 7-12 km (depending on assumed pre-folding thickness of the Hochstegen Fm. of 184-250 m).

The displacement on the Ahorn shear zone is sinistral oblique, with a significant south-side-up offset indicated by differing deformation mechanisms on each side of the shear zone (Rosenberg and Schneider, 2008) and by fission track data (Most, 2003). This coincides with the WSW-plunging sinistral shear sense indicators within the Ahorn shear zone. However, in the Schöberspitzen antiform the shear sense changes from sinistral south-side-up to sinistral north-side-up. This situation can be explained with the model of a positive flower structure which evolves at the transition of a transpressional sinistral shear zone from basement rocks (Zentralgneis) to the metasedimentary cover rocks (Schieferhülle). The Schöberspitzen antiform exhibits the squeezing out of cover rocks from the inner part of western TW westward and upward to the nascent space below the BNF during sinistral transpressive shear (Fig. 13).

The interference patterns of NW/N-plunging and E/ENE-W/WSW-striking folds can be explained in this context too: Folds with NW/N-plunging axes are primarily related to the oblique sinistral shear between the different Zentralgneis bodies and between the Zentralgneis and LSH. These folds are interpreted as part of that group whose axes plot along a great circle parallel to the surface of the Zentralgneis (e.g.: Fig. 11e, f). On the other hand, E/ENE-W/WSW-striking folds are developed mainly within the USH. The latter can be interpreted as fold structures normal to regional shortening (N/NNW-S/SSE), developed in a relatively homogeneous rock mass outside of the major fault zones. Interference patterns of these folds occur mainly in the realm of the Schöberspitzen fold, where large scale detachment folding has lifted rock masses from one into the other deformation regime. Therefore, the interference pattern of folds should be interpreted as the outcome of progressive deformation during one deformation phase rather than a result of two consecutive deformation phases as suggested by Feijth et al. (2007).

The structural link between sinistral shear and folding yields time constraints for the latter, as previously mentioned by Rosenberg and Schneider (2008). Sinistral transpressive shear is linked to the exhumation of the TW (Behrmann, 1988; Selverstone, 1988; Ratschbacher et al., 1991; Wang and Neubauer, 1998), therefore a maximum age of activity is given by the onset of exhumation of the TW (von Blanckenburg et al., 1989: 20 Ma; Frisch et al., 2000: 23 Ma; Selverstone et al., 1995: ≤ 30 Ma). At the SEMP, sinistral strike-slip is well documented since ca. 17 Ma by major subsidence in the Vienna pull-apart basin at the eastern end of the fault system (Ratschbacher et al., 1991). A jump in apatite fission track ages across the Ahorn shear zone south of Hintertux, from about 13 Ma north of the shear zone to about 7 Ma south of it, indicates displacement along the Ahorn shear zone at least until Late Miocene times (Most, 2003; Most et al., 2003). Schneider et al. (2010) provide direct ages (Ar/Ar) for sinistral shearing along shear zones in the western Tauern Window, including the Ahorn shear zone, by determining cooling or growing ages of pre-, syn- and post-kinematic phengites: The authors conclude that "sinistral shear in the western TW started at least 24 Ma ago and terminated at 12 Ma". Although time constraints for major fault zones are not yet very distinct, it is obvious that the period of activity on the Ahorn shear zone overlaps to some extent with the period of activity on the TNBF and the BNF (see also section 6.1.).

7. Conclusion

The Ahorn shear zone is one segment of the western splay of the SEMP within the Tauern Window. At its western end the ENE-striking shear zone passes into a detachment fold with a W-dipping fold axis – called the Schöberspitzen anti-form. The structure can be interpreted as an oblique positive flower structure, which is developed in metasedimentary co-ver rocks (Schieferhülle) above an oblique strike-slip fault in basement rocks (Zentralgneis). An at least 7-12 km offset has been accommodated by the detachment fold.

The recently N-dipping, apparent sinistral Tauern Northern Boundary Fault (TNBF) is interpreted as a rotated, originally WSW-dipping normal fault, which was presumably active during an early stage of the exhumation of the Tauern Window. Therefore, the fault would represent an old part of the normal faulting system at the western margin of the emerging tectonic window. In the course of amplification of the TW the TNBF was increasingly tilted and upright folded. This terminates major activity on the TNBF during Mid-Miocene times while normal faulting on the BNF continued (Fig. 12).

At the transition from the Ahorn shear zone to the Schöberspitzen antiform the direct link between sinistral shearing and upright folding in a transpressional regime can be identified. Time constraints indicate normal faulting (TNBF and BNF) in higher levels of the orogen contemporaneously to the sinistral

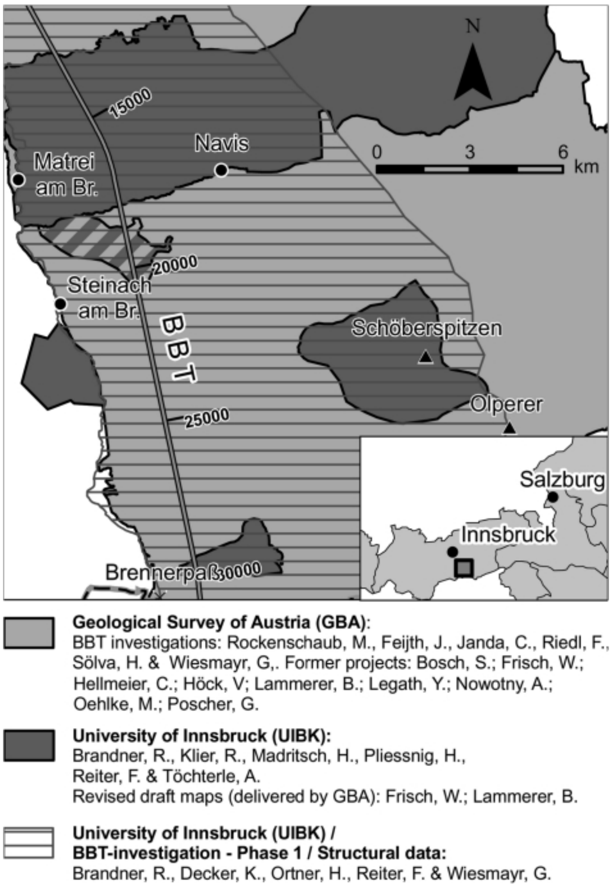

Figure 15: Working groups in the southern Austrian part of BBT investigation area.

transpressive shear in the depth. Strain partitioning between structures at different structural levels can therefore be observed during updoming of the Tauern Window (Fig. 12 & 13). Different structural features in the western TW are seen as a result of their position within the nappe stack and the confining conditions of the particular rock mass, rather than as the outcome of consecutive deformation phases related to differing far-field stresses.

Acknowledgements

We are grateful to the Brenner Basistunnel SE for funding the research projects. In Austria geological investigations were done by the Geological Survey of Austria (GBA) and the University of Innsbruck (UIBK). In addition there are various datasets from three decades of investigation concerning a tunnel below the Brenner Pass. Fig. 15 shows the mapping areas of various working groups and their members, sincere thanks are given to them all. Borehole-televiewing, calculations, and data visualisation were done by the geophysical research company DMT (Essen, Germany). Geophysical data were represented in unpublished geophysical reports for the BBT SE. This study shows some results from these reports and discusses their geological implications. We thank Helena Rodnight, University of Innsbruck, for checking the English. Many thanks also to Walter Kurz and Claudio Rosenberg for their constructive reviews.

References

Behrmann, J.H., 1988. Crustal-scale extension in a convergent orogen: the Sterzing-Steinach mylonite zone in the Eastern Alps. Geodinamica Acta, 2, 63-73.

Behrmann, J.H., 1990. Zur Kinematik der Kontinentalkollision in den Ostalpen. Geotektonische Forschungen, 76, 1-180.

Brandner, R., 1980. Tektonische Übersichtskarte von Tirol. Universitätsverlag Wagner, Innsbruck.

Brandner, R., Reiter, F. and Töchterle, A., 2008. Überblick zu den Ergebnissen der geologischen Vorerkundung für den Brenner-Basistunnel. Geo.Alp, 5, 165-174.

De Vecchi, G. and Baggio, P., 1982. The Pennine zone of the Vizze region, in the Western Tauern Window (Italian Eastern Alps). Bollettino della Società Geologica Italiana, 101, 89-116.

Decker, K. and Reiter, F., 2006. Depth-extrapolated models of fracture orientation and fracture density for the Brenner Base Tunnel. In: M. Tessadri-Wackerle (ed.), Pangeo Austria 2006. innsbruck university press, pp. 44-45.

Dingeldey, C., Dallmeyer, R.D., Koller, F. and Massonne, H.-J., 1997. P–T–t history of the Lower Austroalpine nappe complex in the "Tarntaler Berge" NW of the Tauern Window: implications for the geotectonic evolution of the central Eastern Alps. Contributions to Mineralogy and Petrology, 129, 1-19.

Feijth, J., Rockenschaub, M. and Janda, C., 2007. From subduction to exhumation: interpretation of fold interference in the NW Tauern Window. Geophysical Research Abstracts, 9, EGU2007-A-10322.

Frank, W., Hoinkes, G., Purtscheller, F. and Thöni, M., 1987. The Austroalpine Unit West of the Hohe Tauern: The Ötztal-Stubai Complex as an Example for the Eoalpine Metamorphic Evolution. In: H.W. Flügel and P. Faupl (eds.), Geodynamics of the Eastern Alps.

Frey, M., Desmons, J. and Neubauer, F., 1999. Metamorphic maps of the Alps. Schweizerische Mineralogische und Petrographische Mitteilungen 79.

Frisch, W., 1975. Ein Typ-Profil durch die Schieferhülle des Tauernfensters: Das Profil am Wolfendorn (westlicher Tuxer Hauptkamm, Tirol). Verhandlungen der Geologischen Bundesanstalt, 1974, 201-221.

Frisch, W., Dunkl, I. and Kuhlemann, J., 2000. Post-collisional orogen-parallel large-scale extension in the Eastern Alps. Tectonophysics, 327, 239-265.

Frisch, W., Kuhlemann, J., Dunkl, I. and Brügel, A., 1998. Palinspastic reconstruction and topographic evolution of the Eastern Alps during late Tertiary tectonic extrusion. Tectonophysics, 297, 1-15.

Fügenschuh, B., Mancktelow, N. and Seward, D., 2000. Cretaceous to Neogene cooling and exhumation history of the Oetztal-Stubai basement complex, eastern Alps: A structural and fission track study. Tectonics, 19, 905-918.

Fügenschuh, B., Seward, D. and Mancktelow, N., 1997. Exhumation in a convergent orogen: the western Tauern window. Terra nova, 9, 213-217.

Grundmann, G. and Morteani, G., 1985. The Young Uplift and Thermal History of the Central Eastern Alps (Austria / Italy), Evidence from Apatite Fission Track Ages. Jahrbuch der Geologischen Bundesanstalt, 128, 197-216.

Heidorn, R., Neubauer, F. and Genser, J., 2003a. Structural evolution along the NW margin of the Tauern Window and the relationship to the Geier-Reckner ophiolite-like complex (Eastern Alps, Austria). Memorie di Scienze Geologiche, 54, 213-216.

Heidorn, R., Neubauer, F., Genser, J. and Handler, R., 2003b. 40Ar/39Ar mica age constraints for the tectonic evolution of the Lower Austroalpine to Penninic nappe boundary, Austria. Memorie di Scienze Geologiche, 54, 217-220.

Hoinkes, G., Koller, F., Rantitsch, G., Dachs, E., Höck, V., Neubauer, F. and Schuster, R., 1999. Alpine metamorphism of the Eastern Alps. Schweizerische Mineralogische und Petrographische Mitteilungen, 79, 155-181.

Kießling, W. and Zeiss, A., 1992. New Palaeontological Data from the Hochstegen Marble (Tauern Window, Eastern Alps). Geologisch-Paläontologische Mitteilungen Innsbruck, 18, 187-202.

Klebelsberg, R., 1940. Ein Ammonit aus dem Hochstegenkalk des Zillertales. Zeitschrift der Deutschen Geologischen Gesellschaft, 92, 582-586.

Klier, R., 2005. Das Tarntal Mesozoikum. Diploma thesis, Universität Innsbruck, Innsbruck, 113 pp.

Kurz, W., Unzog, W., Neubauer, F. and Genser, J., 2001. Evolution of quartz microstructures and textures during polyphase deformation within the Tauerm Window (Eastern Alps). International Journal of Earth Sciences, 90, 361-378.

Lammerer, B., 1988. Thrust-regime and transpression-regime tectonics in the Tauern Window (Eastern Alps). Geologische Rundschau, 77, 143-156.

Lammerer, B., Gebrande, H., Lüschen, E. and Veselá, P., 2008. A crustal-scale cross-section through the Tauern Window (eastern Alps) from geophysical and geological data. In: S. Siegesmund, B. Fügenschuh and N. Froitzheim (eds.). Tectonic Aspects of the Alpine-Dinaride-Carpathian System, pp. 219-229.

Lammerer, B. and Weger, M., 1998. Footwall uplift in an orogenic wedge: the Tauern Window in the Eastern Alps of Europe. Tectonophysics, 285, 213-230.

Linzer, H.G., Decker, K., Peresson, H., Dell'Mour, R. and Frisch, W., 2002. Balancing lateral orogenic float of the Eastern Alps. Tectonophysics, 354, 211-237.

Mancktelow, N.S., Stöckli, D.F., Grollimund, B., Müller, W., Fügenschuh, B., Viola, G., Seward, D. and Villa, I.M., 2001. The DAV and Periadriatic fault system in the Eastern Alps south of the Tauern window. International Journal of Earth Sciences, 90, 593-622.

Meisel, T., Melcher, F., Tomascak, P., Dingeldey, C. and Koller, F., 1997. Re–Os isotopes in orogenic peridotite massifs in the Eastern Alps, Austria. Chemical Geology, 143, 217-229.

Miller, H., Ledoux, H., Brinkmeier, I. and Beil, F., 1984. Der Nordwestrand des Tauernfensters - stratigraphische Zusammenhänge und tektonische Grenzen. Zeitschrift der Deutschen Geologischen Gesellschaft, 135, 627-644.

Mitra, S. and Namson, J.S., 1989. Equal-area balancing. American Journal of Science, 289, 563-599.

Most, P., 2003. Late Alpine cooling histories of tectonic blocks along the central part of the Transalp-Traverse (Inntal – Gadertal): constraints from geochronology. PhD thesis, Universität Tübingen, Tübingen, 97 pp.

Most, P., Dunkl, I. and Frisch, W., 2003. Fission track tomography of the Tauern Window along the TRANSALP profile. Memorie di Scienze Geologiche, 54, 225-226.

Müller, W.H. and Briegel, U., 1978. The rheological behaviour of polycrystalline anhydrite. Eclogae Geologicae Helvetiae, Swiss Journal of Geosciences, 71, 397-407.

Passchier, C.W. and Trouw, R.A.J., 2005. Microtectonics. Springer, Berlin, 366 pp.

Pfiffner, O.A., 2009. Geologie der Alpen. Haupt UTB, Bern, 359 pp.

Pliessnig, H., 2008. Zur Stratigraphie der Kaserer-Fm. und zum Abtauchen der "Schöberspitzen-Trias"-Faltenstruktur im Bereich Wildlahnertal und Luftbildauswertung geomorphologischer Geländeformen im südöstlichen Wipptal zwischen Navis und Brenner Diploma thesis, Universität Innsbruck, Innsbruck, 121 pp.

Ratschbacher, L., Dingeldey, C., Miller, C., Hacker, B.R. and McWilliams, M.O., 2004. Formation, subduction, and exhumation of Penninic oceanic crust in the Eastern Alps: time constraints from 40Ar/39Ar geochronology. Tectonophysics, 394, 155-170.

Ratschbacher, L., Frisch, W., Linzer, H.G. and Merle, O., 1991. Lateral extrusion in the eastern Alps, part 2: Structural analysis. Tectonics, 10, 257–271.

Reiter, F., Lenhardt, W.A. and Brandner, R., 2005. Indications for activity of the Brenner Normal Fault zone (Tyrol, Austria) from seismological and GPS data. Austrian Journal of Earth Sciences, 97, 16-23.

Rosenberg, C.L. and Garcia, S., in press. Estimating displacement along the Brenner Fault and orogen-parallel extension in the Eastern Alps. International Journal of Earth Sciences.

Rosenberg, C.L. and Schneider, S., 2008. The western termination of the SEMP Fault (eastern Alps) and its bearing on the exhumation of the Tauern Window. In: S. Siegesmund, B. Fügenschuh and N. Froitzheim (eds.), Tectonic aspects of the Alpine-Dinaride-Carpathian system. Geological Society London Special Publications, pp. 197-218.

Rübel, A., 2006a. Bohrungen - Bereich Navistal-Pfons Bohrung Na-B-01/04s 2/2 Bohrlochgeophysikalische Messungen. BBT report, DMT, Essen, 59 pp.

Rübel, A., 2006b. Bohrungen - Bereich Navistal-Pfons Bohrung Pf-B-01/04s 2/2 Bohrlochgeophysikalische Messungen. BBT report, DMT, Essen, 61 pp.

Rübel, A., 2006c. Bohrungen - Bereich Navistal-Pfons Bohrung Pf-B-02/04 Bohrlochgeophysikalische Messungen. BBT report, DMT, Essen, 57 pp.

Rübel, A., 2006d. Bohrungen - Bereich Navistal-Pfons Bohrung Pf-B-04/05 Bohrlochgeophysikalische Messungen. BBT report, DMT, Essen, 51 pp.

Schmid, S.M., Fügenschuh, B., Kissling, E. and Schuster, R., 2004. Tectonic map and overall architecture of the Alpine orogen. Eclogae Geologicae Helvetiae, Swiss Journal of Geosciences, 97, 93-117.

Schneider, S., Hammerschmidt, K. and Rosenberg, C.L., 2010. Dating the Duration and Termination of Sinistral Shear in the Western Tauern Window: Implications for Indentation and Exhumation in the Eastern Alps. Geophysical Research Abstracts, 12, EGU2010-13949-3.

Selverstone, J., 1985. Petrologic constraints on imbrication, metamorphism, and uplift in the Tauern Window, Eastern Alps. Tectonics, 4, 687-704.

Selverstone, J., 1988. Evidence for east-west crustal extension in the eastern Alps: Implications for the unroofing history of the Tauern window. Tectonics, 7, 87-105.

Selverstone, J., Axen, J.A. and Bartley, J.M., 1995. Fluid inclusion constraints on the kinematics of footwall uplift beneath the Brenner Line normal fault, eastern Alps. Tectonics, 14, 264-278.

Steffen, K.J. and Selverstone, J., 2006. Retrieval of P-T information from shear zones: thermobarometric consequences of changes in plagioclase deformation mechanisms. Contributions to Mineralogy and Petrology, 151, 600-614.

Stipp, M., Stünitz, H., Heilbronner, R. and Schmid, S.M., 2002a. Dynamic recrystallization of quartz: correlation between natural and experimental conditions. In: S. De Meer, M.R. Dryry, J.H.P. De Bresser and G.M. Pennock (eds.), Deformation Mechanisms, Rheology and Tectonics: Current Status and Future Perspectives. Geological Society London Special Publications, pp. 171-190.

Stipp, M., Stünitz, H., Heilbronner, R. and Schmid, S.M., 2002b. The eastern Tonale fault zone: a „natural laboratory“ for crystal plastic deformation of quarz over a temperature range from 250 – 700°C. Journal of Structural Geology, 24, 1861-1884.

Trümpy, R., 1992. Ostalpen und Westalpen - Verbindendes und Trennendes. Jahrbuch der Geologischen Bundesanstalt, 135, 875-882.

Wagreich, M., 1995. Subduction tectonic erosion and Late Cretaceous subsidence along the northern Austroalpine margin (Eastern Alps, Austria). Tectonophysics, 242, 63-78.

Wang, X. and Neubauer, F., 1998. Orogen-parallel strike-slip faults bordering metamorphic core complexes: the Salzach-Enns fault zone in the Eastern Alps, Austria. Journal of Structural Geology, 20, 799-818.

Received: 15 April 2010
Accepted: 11 April 2011

Andreas TÖCHTERLE[*], Rainer BRANDNER & Franz REITER
Institute of Geology and Paleontology, University of Innsbruck, Innrain 52, 6020 Innsbruck, Austria;
[*] Corresponding author, andreas.toechterle@uibk.ac.at